PHILOSOPHICAL TRANSACTIONS OF THE ROYAL SOCIETY A MATHEMATICAL, PHYSICAL & ENGINEERING SCIENCES

Kinematic Dynamo Models

P. H. Roberts

Phil. Trans. R. Soc. Lond. A 1972 **272**, 663-698
doi: 10.1098/rsta.1972.0074

KINEMATIC DYNAMO MODELS

By P. H. ROBERTS†
Advanced Study Program, National Center for Atmospheric Research,‡
Boulder, Colorado, U.S.A.

(*Communicated by Sir Edward Bullard, F.R.S. – Received 4 November* 1971)

CONTENTS

Spherical kinematic dynamo models with axisymmetric magnetic fields are examined, which arise from the mean field electrodynamics of Steenbeck and Krause, and also from the nearly axisymmetric limit of Braginskiĭ. Four main cases are considered: (i) there is no mean flow, but the dynamo is maintained by microscale motions which create a mean electromotive force, $\mathscr{E}$, proportional to the mean magnetic field, $\boldsymbol{B}$ (the α effect); (ii) in addition to an α effect which creates poloidal mean field from toroidal, a mean toroidal shearing flow (angular velocity ω) is present which creates toroidal mean field from poloidal more efficiently than by the α effect; (iii) in addition to the processes operative in (ii), a mean meridional circulation, m, is present; (iv) $\mathscr{E}$ is produced by a second order inductive process first isolated by Rädler. When these processes are sufficiently strong, they can maintain magnetic fields. The resulting situations are known as (i) α^2 dynamos, (ii) $\alpha\omega$ dynamos, (iii) $\alpha\omega$ dynamos with meridional circulations, and (iv) Rädler dynamos.

Models of each type are considered below, but cases (ii) and (iii) give rise to particularly interesting results. If $|m|$ is sufficiently small, or zero [case (ii)], the most easily excited dynamo is oscillatory and is of dipole type if $\alpha\omega' < 0$ in the northern hemisphere (and negative in the southern); here ω' denotes the outward gradient of ω. The oscillation resembles a Parker dynamo wave, generated at the poles, absorbed at the equator and always moving towards lower latitudes, as for the butterfly diagrams of sunspots. If $\alpha\omega' > 0$ in the northern hemisphere, the direction of wave motion is reversed, and also the quadrupolar solution is more readily excited than the dipolar.

If $|m|$ is sufficiently large, and of the right magnitude and sense (which is model dependent), it is found that the dynamo which regenerates most easily is steady. It is of dipolar form if $\alpha\omega' > 0$ but quadrupolar if $\alpha\omega' < 0$. These models appear to be relevant to the Earth, where meridional circulations might be provided by, for example, Ekman pumping.

Evidence for a remarkable symmetry property is adduced. If m and $\alpha\omega'$ are reversed everywhere in the state in which the dipole (say) is most readily excited, it is found that the state in which a quadrupole is most easily regenerated is recovered, almost precisely. Moreover, the critical magnetic Reynolds number for each is closely similar. As a corollary, the critical Reynolds numbers for dipolar and quadrupolar solutions of opposite $\alpha\omega'$ are nearly identical for the $\alpha\omega$ dynamo ($m = 0$).

† Now at School of Mathematics, University of Newcastle upon Tyne.
‡ The National Center for Atmospheric Research is sponsored by the National Science Foundation.

Vol. 272. A. 1230. (Price £1.00; U.S. $2.80) 60 [Published 17 August 1972

1. Introduction

The kinematic dynamo problem is that of determining, whether a flow, $\boldsymbol{u}$, assigned within a body, V, of conducting fluid, can amplify or maintain a magnetic field, $\boldsymbol{B}$, within it, without the need for external sources of field. The mathematical question centres on solutions of the pre-Maxwell equations

$$\operatorname{curl} \boldsymbol{E} = -\partial \boldsymbol{B}/\partial t, \quad \operatorname{curl} \boldsymbol{B} = \mu \boldsymbol{j}, \quad \operatorname{div} \boldsymbol{B} = 0, \tag{1.1}$$

and Ohm's law

$$\boldsymbol{j} = \sigma(\boldsymbol{E} + \boldsymbol{u} \times \boldsymbol{B}), \tag{1.2}$$

in its form suitable for a moving conductor (see, for example, Roberts 1967*a*). Here μ and σ are the permeability and conductivity of the fluid both assumed constant; m.k.s. units are used. If, as in the case considered here, the fluid is bounded by a fixed surface, S, which separates it from an insulator, V, we must have

$$\langle \boldsymbol{B} \rangle = 0 \quad \text{on} \quad S, \tag{1.3}$$

where $\langle Q \rangle$ denotes the leap in the quantity Q across the surface. The condition that the dynamo is not maintained externally becomes

$$|\boldsymbol{B}| = O(r^{-3}) \quad (r \to \infty), \tag{1.4}$$

where r denotes distance from some origin in V. The condition that the field does not decay with time is

$$|\boldsymbol{B}| \not\to 0, \quad t \to \infty, \tag{1.5}$$

and is written in this way to emphasize that oscillatory dynamos are not excluded.

This completes the specification of the mathematical problem. The induction equation follows from (1.1) and (1.2), namely

$$\partial \boldsymbol{B}/\partial t = \operatorname{curl}(\boldsymbol{u} \times \boldsymbol{B}) + \eta \nabla^2 \boldsymbol{B}, \tag{1.6}$$

where

$$\eta = 1/\mu\sigma \tag{1.7}$$

is the magnetic diffusivity.

It is known that no fields obeying (1.4) to (1.6) exist if $\boldsymbol{B}$ is axisymmetric (Cowling 1933), or if $\boldsymbol{u}$ is toroidal (Bullard & Gellman 1954), or if rates of strain $\partial u_i/\partial x_j$ are too small (Backus 1958), or if $\boldsymbol{u}$ itself is too small (Childress 1969), as measured by the magnetic Reynolds number

$$R = \mathscr{U} a/\eta, \tag{1.8}$$

where $\mathscr{U}$ is a typical flow speed, and a a typical dimension of V. In view of all these negative results, it is comforting to know that solutions evading these theorems do exist; Lortz (1968) provided a particularly neat example.

It has become apparent that motions which lack mirror symmetry are efficient in field regeneration (Steenbeck & Krause 1966; Childress 1967, 1969, 1970). A rough measure of the degree of mirror symmetry is the quantity $\boldsymbol{u} \cdot \operatorname{curl} \boldsymbol{u}$, but it should be noted that motions exist in which this quantity vanishes on average, even though mirror symmetry is absent, and dynamo action can occur (Rädler 1969*a*, *b*, 1970).

In the geophysical or cosmical context, the numerous, rigorously constructed, models of working dynamos which now exist generally involve containers V of unrealistic shape, or postulate fluid motions which are unrealistic in their spatial or temporal behaviour. Those not suffering from these objections have been investigated by numerical means and have generally shown

a disappointing† rate of convergence (Lilley 1970), or no signs of convergence whatever (e.g. Bullard & Gellman 1954; Gibson & Roberts 1969). [An exception is the numerical study by G. O. Roberts (unpublished; reported by Roberts 1971*a*) of the excitation of asymmetric fields by symmetric motions. Such flows are probably not, however, highly significant in the cosmical applications.] For this reason, the subject has developed two main branches which are more closely tied to nature.

The first approach, pioneered by Parker (1955) and greatly developed by Steenbeck, Krause, and Rädler (cf. Roberts & Stix 1971), is the turbulent dynamo. The fluid velocity, $\boldsymbol{u}$, and therefore $\boldsymbol{B}$ also, may be divided into mean parts ($\bar{\boldsymbol{u}}$ and $\bar{\boldsymbol{B}}$) and fluctuating parts, by writing

$$\boldsymbol{u} = \bar{\boldsymbol{u}} + \boldsymbol{u}', \quad \boldsymbol{B} = \bar{\boldsymbol{B}} + \boldsymbol{B}', \tag{1.9}$$

the averages being taken over an ensemble of identical systems. A new subject is developed, named 'mean field electrodynamics' by Steenbeck, Krause, and Rädler, in which the relation between the mean fields is studied and the possibility of dynamo maintenance of these fields is examined. Even as a study of the microscale in classical electrodynamics reveals the presence of new terms (e.g. the electric and magnetic polarizations) which affect the macroscopic (averaged) fields, so the presence of turbulence will affect the mean fields $\bar{\boldsymbol{B}}$, $\bar{\boldsymbol{E}}$, $\bar{\boldsymbol{j}}$, etc. Since Maxwell's equations (1.1) are linear, these hold as before, when the overbars are added. Ohm's law (1.2), however, acquires a new term on averaging. We obtain

$$\bar{\boldsymbol{j}} = \sigma(\bar{\boldsymbol{E}} + \bar{\boldsymbol{u}} \times \bar{\boldsymbol{B}} + \bar{\boldsymbol{\mathscr{E}}}), \tag{1.10}$$

where

$$\bar{\boldsymbol{\mathscr{E}}} \equiv \overline{\boldsymbol{u}' \times \boldsymbol{B}'} \tag{1.11}$$

will be referred to as 'the mean electromotive force'. This may be evaluated by examining induction on the microscale, and can be exhibited as a linear functional of $\bar{\boldsymbol{B}}$, whose properties can be illuminated both by general arguments, and by expansion methods (see, for example, Roberts 1971*b* or Roberts & Stix 1971). A particularly interesting case is that in which the motion lacks mirror symmetry, i.e. in which, according to the felicitious word coined by Moffatt (1969), the flow possesses 'helicity'. (Parker (1955) called turbulence having this property 'cyclonic'.) In this case $\bar{\mathscr{E}}_i$ will in general be well represented by a linear combination $a_{ij}\bar{B}_j$ of the components of $\bar{\boldsymbol{B}}$. Moreover, whether it lacks mirror symmetry or not, terms linear in $\partial \bar{B}_i/\partial x_j$ will also occur, which will enhance the diffusivity η as far as the mean field is concerned. A particularly simple, and easily apprehended, form of $\bar{\boldsymbol{\mathscr{E}}}$ is provided by the case of isotropic, non-mirror-symmetric turbulence, for which the linear combination $a_{ij}\bar{B}_j$ reduces to $\alpha\bar{B}_j$. This new term in Ohm's law for $\bar{\boldsymbol{j}}$ has been termed 'the α effect' by Steenbeck, Krause, and Rädler.

The second main approach, pioneered by Braginskiĭ (1964*a*, *b*), is through the nearly symmetric dynamo. Symmetric fields, $\boldsymbol{B}$, cannot be maintained indefinitely, but there is no reason why nearly symmetric fields should not be sustained, by a fluid motion which, also, is nearly symmetric. Of course, it may be expected that a large Reynolds number, R, will be required for dynamo action, so a double limit is considered in which $R \to \infty$ and, simultaneously the degree of asymmetry approaches zero. The mathematical attractions of the scheme are great. Not only have such singular perturbation problems been extensively studied in the context of the boundary layer, but also the 'frozen field' picture (appropriate to the case $R = \infty$) is useful except in the magnetic diffusion layers on the surface of V. Moreover, the fields of the Earth and Sun (to quote

† With the greater power of the CDC 7600 computer at the National Center for Atmospheric Research, the present author was able to examine higher truncation levels than Lilley. He found that the verisimilitude of convergence in table 5 of Lilley (1970) was largely illusory. He also examined other flows for which (unlike Lilley's choice) the rates of strain were everywhere finite, but obtained no convincing convergence.

two examples) are primarily axisymmetric. Of course, it may be urged that the degree of asymmetry, though small, is finite and that an $R \to \infty$ limit is therefore not appropriate. But one might just as well argue that the limit of infinite Reynolds number is never reached in a practical boundary layer, and that therefore boundary-layer theory is useless, and we ignore this objection. If now the overbar above is taken to mean an average over ϕ, the polar angle about the axis of symmetry, (1.10) and (1.11) apply. Moreover, it is remarkable that (to leading order in the expansion in the asymmetries) $\bar{\mathscr{E}}$ is proportional to $\bar{\boldsymbol{B}}_\phi$, the ϕ component of $\bar{\boldsymbol{B}}$ (provided certain effective fields are introduced; see also Soward (1971)). Further, the constant, α, of proportionality can be explicitly calculated from the asymmetric flow, $\boldsymbol{u}'$, assumed, and is closely related to the helicity of the flow (Soward 1972).

The present paper is mainly concerned with investigating some of the consequences of the α effect on symmetric fields. (Except at the beginning of § 6, the overbars will henceforward be omitted.) Several such models have been constructed by Krause & Steenbeck (see Roberts & Stix 1971) and also by Braginskiĭ (1964*b*) and Parker (1955, 1971*a*, *b*, *c*). In § 2 the basic formalism is developed from the expansion method of Bullard & Gellman (1954). In § 3 dynamos functioning by α effect alone are examined, in § 4 the effect of azimuthal shear is included, and in § 5 meridional circulations are added. In § 6 a different aspect of mean field electrodynamics, which also has its counterpart in higher terms of the Braginskiĭ expansion (Soward 1972), is examined by a model proposed by Rädler (1969*b*, 1970).

2. Mathematical formulation

We adopt the formalism of Bullard & Gellman (1954) which is particularly convenient for dealing with (1.3) and (1.4) when V is a sphere, the case considered here. Let (r, θ, ϕ) be spherical polar coordinates with origin at the centre of the sphere (radius a), and $\theta = 0$ the axis of symmetry of the fields sought. We include $\mathscr{E}$ as $\alpha \boldsymbol{B}$ in (1.6), and write the resulting equation in scaled form as

$$\Omega \boldsymbol{B} = R \operatorname{curl} (\boldsymbol{u} \times \boldsymbol{B} + \alpha \boldsymbol{B}) + \nabla^2 \boldsymbol{B}, \tag{2.1}$$

where a is the unit of length, a^2/η (the electromagnetic diffusion time) is the unit of time, and R is given by (1.8). Since we will seek the normal mode solutions of (2.1), we have replaced the $\partial \boldsymbol{B}/\partial t$ of (1.6) by $\Omega \boldsymbol{B}$, where Ω is the (complex) growth rate of the field in units of η/a^2.

We expand $\boldsymbol{B}$ and $\boldsymbol{u}$ in the forms

$$\boldsymbol{B} = \operatorname{curl} T\hat{\boldsymbol{r}} + \operatorname{curl}^2 S\hat{\boldsymbol{r}}, \tag{2.2}$$

$$\boldsymbol{u} = \operatorname{curl} t\hat{\boldsymbol{r}} + \operatorname{curl}^2 s\hat{\boldsymbol{r}}, \tag{2.3}$$

where $\hat{\boldsymbol{r}}$ is the unit radial vector. [Since time has now been suppressed in favour of Ω, the use of t in (2.3) should not cause confusion.] The functions T, S, t, s and α may be divided into spherical harmonic components as

$$T = \sum_{e,\,o} T_n(r) P_n(\theta), \qquad S = \sum_{o,\,e} S_n(r) P_n(\theta), \tag{2.4}$$

$$t = \sum_{1,3,5,\ldots} t_n(r) P_n(\theta), \quad s = \sum_{2,4,6,\ldots} s_n(r) P_n(\theta), \tag{2.5}$$

$$\alpha = \sum_{1,3,5,\ldots} A_n(r) P_n(\theta), \tag{2.6}$$

where P_n denotes the Legendre polynomial of degree n. The assumption of odd n terms in α and t, and even n terms in s is quite natural from the dynamical point of view. It implies that (in Cartesian coordinates x, y, z) α and $\boldsymbol{u}$ at the reflected point $\boldsymbol{x}_R = (x, y, -z)$ in the equatorial plane are

$$\boldsymbol{u}(\boldsymbol{x}_R) = [u_x(\boldsymbol{x}), u_y(\boldsymbol{x}), -u_z(\boldsymbol{x})], \quad \alpha(\boldsymbol{x}_R) = -\alpha(\boldsymbol{x}). \tag{2.7}$$

For $\boldsymbol{u}$ and α with this parity it is possible to seek $\boldsymbol{B}$ with the same or opposite parity. Solutions in which the set $e = \{2, 4, 6, \ldots\}$ of even n is assumed for T in (2.4) and the set $o = \{1, 3, 5, \ldots\}$ of odd n is assumed for S satisfy

$$\boldsymbol{B}(\boldsymbol{x}_R) = [-B_x(\boldsymbol{x}), -B_y(\boldsymbol{x}), B_z(\boldsymbol{x})], \tag{2.8}$$

and are later referred to as 'solutions of dipole type'. If, instead, o is selected for T and e for S, it is found that

$$\boldsymbol{B}(\boldsymbol{x}_R) = [B_x(\boldsymbol{x}), B_y(\boldsymbol{x}), -B_z(\boldsymbol{x})]. \tag{2.9}$$

These will be said to be of 'quadrupole type'.

Adopting, modifying and extending the notation and procedure of Bullard & Gellman (1954), we may combine (2.1) to (2.6) to give

$$\Omega S_\gamma = R \sum_{\alpha\beta} [(s_\alpha S_\beta S_\gamma) + (A_\alpha T_\beta S_\gamma)] + \nabla_\gamma^2 S_\gamma, \tag{2.10}$$

$$\Omega T_\gamma = R \sum_{\alpha\beta} [(s_\alpha T_\beta T_\gamma) + (t_\alpha S_\beta T_\gamma) + (A_\alpha S_\beta T_\gamma)] + \nabla_\gamma^2 T_\gamma, \tag{2.11}$$

where

$$\nabla_\gamma^2 = \frac{\mathrm{d}^2}{\mathrm{d}r^2} - \frac{n_\gamma(n_\gamma+1)}{r^2}. \tag{2.12}$$

Here α, β and γ denote any relevant triad of n indices, and a bracket, such as $(t_\alpha S_\beta T_\gamma)$, denotes the action of the component t_α of flow on the S_β component of field to produce a T_γ component of field. It may be shown that

$$N_\gamma(s_\alpha S_\beta S_\gamma) = \left[p_\alpha c_\alpha \frac{s_\alpha}{r^2}\frac{\mathrm{d}S_\beta}{\mathrm{d}r} - p_\beta c_\beta \frac{S_\beta}{r^2}\frac{\mathrm{d}s_\alpha}{\mathrm{d}r}\right] G_{\alpha\beta\gamma}, \tag{2.13}$$

$$N_\gamma(s_\alpha T_\beta T_\gamma) = \left[p_\alpha c_\alpha \frac{\mathrm{d}}{\mathrm{d}r}\left(\frac{s_\alpha T_\beta}{r^2}\right) + p_\gamma c_\gamma \frac{T_\beta}{r^2}\frac{\mathrm{d}s_\alpha}{\mathrm{d}r}\right] G_{\alpha\beta\gamma}, \tag{2.14}$$

$$N_\gamma(t_\alpha S_\beta T_\gamma) = -\left[p_\beta c_\beta \frac{\mathrm{d}}{\mathrm{d}r}\left\{\frac{t_\alpha S_\beta}{r^2}\right\} + p_\gamma c_\gamma \frac{t_\alpha}{r^2}\frac{\mathrm{d}S_\beta}{\mathrm{d}r}\right] G_{\alpha\beta\gamma}, \tag{2.15}$$

$$N_\gamma(A_\alpha T_\beta S_\gamma) = -c_\alpha A_\alpha T_\beta G_{\alpha\beta\gamma}, \tag{2.16}$$

$$N_\gamma(A_\alpha S_\beta T_\gamma) = \left[c_\alpha \frac{\mathrm{d}}{\mathrm{d}r}\left\{A_\alpha \frac{\mathrm{d}S_\beta}{\mathrm{d}r}\right\} + p_\beta p_\gamma \frac{A_\alpha S_\beta}{r^2}\right] G_{\alpha\beta\gamma}, \tag{2.17}$$

where

$$p_\alpha = n_\alpha(n_\alpha+1), \quad c_\alpha = \tfrac{1}{2}(p_\alpha - p_\beta - p_\gamma), \quad \text{etc.} \tag{2.18}$$

$$G_{\alpha\beta\gamma} = \iint Y_\alpha Y_\beta Y_\gamma \sin\theta \,\mathrm{d}\theta \,\mathrm{d}\phi, \tag{2.19}$$

and

$$N_\gamma = \frac{4\pi n_\gamma(n_\gamma+1)}{(2n_\gamma+1)}. \tag{2.20}$$

Equations (2.13) to (2.15) are equivalent to results (24) of Bullard & Gellman, while (2.16) and (2.17) follow from results given by Roberts (1967*b*). The notation (2.19) for the Gaunt integral $G_{\alpha\beta\gamma}$ follows that of Bullard & Gellman, the Y denoting any surface harmonic, here simply a Legendre polynomial P. The Gaunt integral obeys certain selection rules set out by Bullard & Gellman (p. 229). They have been tabulated by Scott (1969), who also lists a number of their properties.

The boundary conditions which must be satisfied by T_γ and S_γ are (Bullard & Gellman, eq. 27)

$$T_\gamma = \frac{\mathrm{d}S_\gamma}{\mathrm{d}r} + \frac{n_\gamma S_\gamma}{r} = 0, \quad \text{at} \quad r = 1. \tag{2.21}$$

If the conductor fills the sphere, T_γ and S_γ must be finite everywhere within it and, in particular,

$$T_\gamma = O(r^{n_\gamma+1}), \quad S_\gamma = O(r^{n_\gamma+1}), \quad (r \to 0) \tag{2.22}$$

(Bullard & Gellman, eq. 28). When subjected to (2.21) and (2.22), equations (2.10) and (2.11) define an eigenvalue problem for Ω, and (since all coefficients are real) if Ω is an eigenvalue, so is its complex conjugate Ω^*. In what follows, we assume always that $\mathrm{Im}\,(\Omega) \geqslant 0$ and ignore Ω^*. When R is zero, Ω belongs to the decay modes of a sphere and is negative. As R is increased, a critical value ($R = R_c$, say) is reached at which $\mathrm{Re}\,(\Omega)$ is zero for one mode and is negative for all others. This defines the critical Reynolds number for dynamo action. Its determination was the primary objective in the calculations which are described later. If R is increased further, $\mathrm{Re}\,(\Omega)$ becomes positive for one (or more) modes. If $\Omega = 0$ at $R = R_c$ for the relevant mode, the dynamo, will be described as a d.c. dynamo, while if $\mathrm{Im}\,(\Omega) \neq 0$ it will be said to be an a.c. dynamo, and the determination of $\mathrm{Im}\,(\Omega)$ becomes a secondary objective of the calculations. From now onwards, the subscript on R_c will be suppressed.

It may be worth observing that the formulation given above is easily extended to other cases. It is a simple matter (Roberts & Stix 1972) to generalize (2.16) and (2.17) to the case of asymmetric fields. The possibility of a spatially varying η is of particular interest for the turbulent dynamo, for which the turbulent diffusivity should depend on the turbulent intensity. If, for example, η depends on r alone, it is only necessary to replace $\eta\nabla_\gamma^2 T_\gamma$ by $\eta\nabla_\gamma^2 T_\gamma + \eta'\,\partial T_\gamma/\partial r$, leaving $\eta\nabla_\gamma^2 S_\gamma$ unaltered (Roberts & Stix 1972). Other sets of boundary calculations are also readily dealt with. If the volume, V, of conducting fluid fills only the shell $f < r < 1$, the core, C, defined by $r \leqslant f$ being insulating, (2.22) is replaced by

$$T_\gamma = \frac{\mathrm{d}S_\gamma}{\mathrm{d}r} - \frac{n_\gamma+1}{r} S_\gamma = 0 \quad \text{at} \quad r = f, \tag{2.23}$$

while if C is a solid of the same conductivity, and the dynamo sought is steady ($\Omega = 0$) we have instead

$$\frac{\mathrm{d}S_\gamma}{\mathrm{d}r} - \frac{n_\gamma+1}{r} S_\gamma = N_\gamma \left[\frac{\mathrm{d}T_\gamma}{\mathrm{d}r} - \frac{n_\gamma+1}{r} T_\gamma\right] - R\sum_{\alpha\beta} c_\alpha A_\alpha \frac{\mathrm{d}S_\beta}{\mathrm{d}r} G_{\alpha\beta\gamma} = 0 \quad \text{at} \quad r = f, \tag{2.24}$$

where, for simplicity we assume $\boldsymbol{u}$ is continuous on $r = f$. If C is a solid conductor but $\Omega \neq 0$, the boundary conditions become intricate but, provided the skin depth

$$\delta \equiv \sqrt{(2/\Omega)} \tag{2.25}$$

is small compared with f, they reduce to those applying to a perfectly conducting C, namely

$$S_\gamma = N_\gamma \frac{\mathrm{d}T_\gamma}{\mathrm{d}r} - R\sum_{\alpha\beta} c_\alpha A_\alpha \frac{\mathrm{d}S_\beta}{\mathrm{d}r} G_{\alpha\beta\gamma} = 0 \quad \text{at} \quad r = f. \tag{2.26}$$

In this case a current skin, of thickness δ, lies at the surface of C.

In the numerical work, we concentrated on the case of the full sphere defined by (2.21) and (2.22). We truncated (2.10) and (2.11) after an equal number, N, of harmonics of S and T, there being $2N$ in all. We divided the range $(0, 1)$ of r into M equal intervals, $r = 1$ being the Mth point, the limit (2.22) being implied in the subsequent difference formulae, as was the condition (2.21) on T_γ. A value for $S(M)$ was, however, stored and was obtained in the following way. Taylor expansion of S_γ, and use of the second of (2.21) gives the estimate

$$(2/h^2)\,\{S_\gamma(M-1) - [1 + n_\gamma h + \tfrac{1}{2} n_\gamma(n_\gamma+1)\,h^2]\,S_\gamma(M)\} \tag{2.27}$$

of

$$[\nabla_\gamma^2 S_\gamma(r)]_{r=1},$$

where $h = 1/M$ is the grid interval. This reduces (2.10) for $r = 1$ to the eigenvalue form

$$Ax = \Omega x, \tag{2.28}$$

into which the remaining finite difference equations arising from (2.10) and (2.11) fall. Here the column vector is composed of $S_\gamma(J)$ for $J = 1$ to M and $T_\gamma(J)$ for $J = 1$ to $M-1$. The matrix A is composed of three or more bands of three elements, and zeros elsewhere.

Non-trivial solutions of (2.28) were obtained for a number of values of N and M, and an attempt was made to obtain convergence as N and M were increased. It was, of course, necessary in the case of oscillatory dynamos that the electromagnetic skin depth, δ, should be large compared with h. For $M = 20$, for example, this meant that values of $|\Omega|$ exceeding about 400 could not be trusted. A number of checks were available. These naturally included the usual decay mode for zero α and a solid body rotation for $\boldsymbol{u}$. Also, comparisons could be made with results reported by Krause & Steenbeck (see, for example, Roberts & Stix (1971)) and Braginskiĭ (1964*b*). These will be described below.

Equation (2.28) was attacked by one of two methods: the QR algorithm and inverse iteration. The advantage of the former method lies in the assurance it gives that the critical value of R obtained in the search for a zero $\mathrm{Re}\,(\Omega)$ is indeed the smallest. Its disadvantage is its extreme slowness, and the fact that it makes no use of the banded structure of A. Because of storage problems, this curtails, at times seriously, the values of N and M which can be attained. The advantage of inverse iteration lies in its speed and in superior storage properties, particularly when real Ω are sought. With the CDC 6600 at the National Center for Atmospheric Research, on which these present calculations of §§ 3 to 6 were performed, the limits on the QR algorithm were effectively $M = 20$ and $N = 10$ for which the matrix A had 195 rows and columns. If the series (2.5) and (2.6) were limited to one harmonic of t and α and none of s, as is the case for the $\alpha\omega$ dynamos examined in § 4, it is possible (if necessary for convergence) to proceed with inverse iteration as far as $M = 20$ and $N = 28$ for complex Ω, for which the matrix A has 546 rows and columns, and a band width of 43. For three of the cases of § 5, for which at least two components of t or two components of α are present, the band width for $M = 20$ is 121 and it is only possible to proceed as far as $N = 10$ for complex Ω, though even then an eigenvalue could be obtained far more rapidly than by the QR algorithm. For the second model of § 5, the band width was only 82 for $M = 20$, and it was possible to obtain solutions for complex Ω at the $N = 14$ truncation level.

3. The α^2 dynamos

It is possible to maintain a large-scale field by the inductive action of turbulence alone, without any help from large-scale motions whatever. The toroidal field generates a toroidal current, by the α effect, and this current creates the poloidal field from which, again through the α effect, the original toroidal field is sustained. Such a dynamo, working on a product of two α effects, will be called here 'an α^2 dynamo'. Naturally, if the α effect is too weak, the regeneration will be insufficient to counter ohmic decay, and the dynamo will fail. In order to obtain regeneration, we require that the α effect Reynolds number,

$$R_\alpha = \alpha_0 a/\eta, \tag{3.1}$$

should attain a certain critical value, where α_0 is some characteristic value of α (here taken to be its maximum value) within the sphere. It was the objective of the calculations reported below to find critical values of R_α for a number of models.

The first model considered was one proposed by Steenbeck & Krause (1966), and is defined by

$$\text{model 1:} \quad \alpha = \alpha_0 \cos\theta. \tag{3.2}$$

The non-analytic behaviour of α at the centre of the sphere is not attractive, but the simplicity of the model permits solution by series expansion without prohibitive labour, and this provides a valuable check against the matrix method used in other cases.

Instead of the expansion (2.4) in Legendre functions, Steenbeck & Krause developed solutions in Fourier series in θ. Although the eigenvalue obtained must, in the limit $N \to \infty$, be independent of which expansion base is chosen, there is, of course, no reason why this should be so for finite N. Remarkably enough, however, the equations governing the dipole family at the $N = 1$ truncation level based on (2.4) coincide (after scaling) with those of Steenbeck & Krause (1966), provided that we set

$$R = \sqrt{5}C, \tag{3.3}$$

where C is the eigenvalue parameter of their theory. On using 20 grid points in r, we obtained the value ± 10.54 for R. Their result of $C = \pm 4.13$ leads, however, to $R = \pm 9.23$. To resolve this discrepancy, we repeated their calculation using their method, and obtained the value, R, for $N = 1$ and $M = \infty$ shown in table 1; this is clearly in excellent accord with the results of the grid point calculation.

TABLE 1. CRITICAL REYNOLDS NUMBERS FOR α^2 DYNAMO OF STEENBECK & KRAUSE

See model 1, equation (3.2)

truncation		Reynolds numbers R	
N	M	dipole	quadrupole
1	20	10.54	11.55
1	40	10.55	11.56
1	∞	10.552	11.567
2	20	7.787	7.995
2	40	7.793	8.002
3	20	7.641	7.809
4	20	7.637	7.803
5	20	7.637	7.803
5	30	7.641	7.808
6	20	7.637	7.803

We also repeated Steenbeck & Krause's calculation for the quadrupole eigenvalue at the $N = 1$ truncation level, obtaining a value of C of ± 4.7979, which is in satisfactory agreement with their values of ± 4.81. Actually, in this case, the equations obtained for the two choices of expansion base differ. [As well as introducing the transformation (3.3), it is necessary to replace the 5 in their eqn (25) by 4.] We also used the set appropriate to the expansion (2.4) to find a solution by the series method used by Steenbeck & Krause. We obtained the value of R for $N = 1$ and $M = \infty$ shown in table 1, which is again in excellent agreement with the results obtained from the grid point method.

Table 1 records the results obtained for various truncation levels and mesh sizes. It appears that the values listed for model 1 in table 2 are good approximations to the eigenvalues sought.

It is interesting to notice that the dynamo is d.c. and not a.c. This was characteristic of the other α^2 dynamos which we examined, and was also noted by Steenbeck & Krause (1969*b*) who argued that the general steadiness of the geomagnetic field, over times long compared with its ohmic diffusion time, might indicate that this field owes its origin to an α^2 dynamo mechanism.

It seems more likely, however, (§ 5) that the steadiness of the Earth's field is a consequence of significant meridional circulations within its core. In any case, some of the arguments presented by Steenbeck & Krause (1969*b*, § A 2; see particularly eqns (7) to (9)) would appear to be debatable.

TABLE 2

model no.	defining equation	dipole eigenvalue	quadrupole eigenvalue	truncation N	truncation M
1	3.2	7.637	7.803	4, 5, 6	20
		7.641	7.808	5	30
2	3.4	24.56	24.54	6, 7	20
		24.95	24.93	5	30
3	3.5	14.10	14.10	5	30
4	3.6	12.96	13.03	4, 5	20
		13.04	13.11	4	30
5	3.7	10.09	10.45	6, 7	20

Two other forms for α which were examined by Steenbeck & Krause (1969*b*) in their study of the geomagnetic dynamo were proportional to

$$\text{model 2:} \quad \alpha = \alpha_0 r(3r-2)\cos\theta, \tag{3.4}$$

$$\text{model 3:} \quad \alpha = 7.376\alpha_0 r^2(1-r)(5r-3)\cos\theta. \tag{3.5}$$

[The constant 7.376 in the latter equation actually represents the more complicated expression $2\sqrt{6}(16-\sqrt{6})/9$ which ensures that, as for the other models considered here, α_0 is the maximum value of α.] The results obtained are listed in table 2. In comparing these results with those of Steenbeck & Krause, it should be noted that, if, as it appears (compare their eqns (2) and (5)), their α is normalized so that its integral from 0 to x has unit maximum, the numerator 125 in their expression at the end of Section D defining model 3 above should be replaced by 3125. Moreover, in making comparisons with the results of table 2, their eigenvalues should be multiplied by 27/4 and $3125/(108\times 7.376)$ for models 2 and 3 respectively [for example, compare their (5) for $x_T = 0$ with (3.4) above]. Taking $N = 6$, they obtained, for model 2, the eigenvalues $R = 25.20$ (dipole) and $R = 25.19$ (quadrupole), while for model 3 they found $R = 14.22$ for both dipole and quadrupole parities. It may be seen that the agreement is quite satisfactory.

Other models were examined almost incidentally as a part of the investigation reported in § 4 below. These were:

$$\text{model 4:} \quad \alpha = \tfrac{729}{16}\alpha_0 r^8(1-r^2)^2\cos\theta, \tag{3.6}$$

$$\text{model 5:} \quad \alpha = 24\sqrt{3}\,\alpha_0 r^2(1-r)^2\cos\theta\sin^2\theta, \tag{3.7}$$

the latter being the only case in which other than the simple sin dependence on latitude was assumed. The results obtained are also listed in table 2.

It is interesting to observe how close the critical Reynolds numbers are for the dipole and quadrupole families. This is particularly true of models 2 to 5, for which α is regular at $r = 0$. Steenbeck & Krause (1969*b*), in commenting on this, observed that the toroidal current systems belonging to the eigensolutions for models 2 and 3 tend to be concentrated in high latitudes. In other words, the mutual inductance of the two hemispheres is, as far as the critical marginal solutions are concerned, small. Thus, the fields and currents in one hemisphere may be reversed, and hence the parity changed, without greatly affecting the growth rate of the solution.

Although this argument illuminates the situation, it does not explain why j_ϕ should be large only near the poles. In this connexion, an argument indicated by Weiss (1971) would appear to shed light. Consider a solution of dipole parity, in which B_ϖ and B_ϕ are odd in z, while B_z and j_ϕ are even, (ϖ, ϕ, z) being cylindrical polar coordinates. In general, B_z will not vanish on the equatorial plane, E, and one might be tempted to infer that j_ϕ is also unlikely to be zero on E. But α and B_ϕ vanish on E, in general linearly with z, and thus, in the steady marginal state, j_ϕ *must* vanish everywhere on E. The paradox is resolved by noting that $\boldsymbol{B}$ can be a potential field on E in the steady state; then B_z will not vanish on E but j_ϕ will. If j_ϕ vanishes linearly in z, it must, because of the chosen parity, vanish quadratically, i.e. to the same order as αB_ϕ, and the contradiction evanesces.

To confirm this reasoning, $|j_\phi(\varpi, \phi, 0)/B_{z,\max}|$ was evaluated numerically everywhere on E for model 1. The ratio was found to be nowhere greater than 1.3×10^{-4} for $N = 6$ and $M = 20$, and nowhere greater than 5×10^{-8} for $N = 9$ and $M = 20$. It seems plausible that, in the limit $N \to \infty$ and $M \to \infty$, it will indeed vanish.

Calculations on dynamos of α^2 type are extremely rapid, the entire set of results obtained here taking only a few minutes of CDC 6600 time. It seems that, for α^2 dynamos generally, qualitatively correct results can be obtained for small values of N.

4. The $\alpha\omega$ dynamos

It is well known that, in addition to the α effect, there is another mechanism by which toroidal field can be created from poloidal field. This is the shearing of lines of force by a large-scale differential rotation, ω. If ω_0' denotes some typical spatial gradient of ω, which in this section we will take to be its maximum value within the sphere, we may define a Reynolds number for shear by

$$R_\omega = \omega_0' a^3/\eta. \tag{4.1}$$

If $R_\omega \gg R_\alpha$, the creation $(A_\alpha S_\beta T_\gamma)$ of toroidal field by the α effect may be neglected in (2.11) in comparison with $(t_\alpha S_\beta T_\gamma)$, its production by the shear, although it is still necessary to invoke the α effect in sustaining the poloidal field. Such a dynamo, working on a product of an α effect and a shear (ω) effect, will be called here 'an $\alpha\omega$ dynamo'. Since field creation by the α effect is here so weak compared with that of the ω effect, the ratio of toroidal to poloidal field is large, of order $(R_\omega/R_\alpha)^{\frac{1}{2}}$ in fact. Naturally, if the product of α and ω effects is too weak, the regeneration will be insufficient to counter ohmic decay, and the dynamo will fail. In order to obtain regeneration, we require that the product of the two Reynolds numbers, or (as we will use here) its square root

$$R = \sqrt{(|R_\alpha R_\omega|)}, \tag{4.2}$$

should attain some critical value. It was the objective of the calculations reported below to find the critical values of R for a number of models.

The $\alpha\omega$ dynamos have a significance beyond the context of the turbulent dynamo. Braginskiĭ's theory of the nearly symmetric dynamo gives rise, to leading order, to $\alpha\omega$ dynamo models (see, for instance, Roberts (1971*b*)). For this reason, Braginskiĭ (1964*b*) undertook some numerical work on this type of dynamo: this will be described in § 5 below.

The first model we considered was one proposed by Steenbeck & Krause (1966), and is defined by

$$\text{model 1:} \quad \alpha = \alpha_0 \cos\theta, \quad \omega = \omega_0' r. \tag{4.3}$$

This model is subject to the advantages and disadvantages outlined below (3.2). The eigenvalue equations at the $N = 1$ truncation level coincide with those obtained by Steenbeck & Krause from their expansions in Fourier series, provided R is related to their eigenvalue parameter, C, by

$$R = \begin{cases} \sqrt{(\frac{5}{4}C)}, \text{ for dipole parity,} \\ \sqrt{(\frac{5}{8}C)}, \text{ for quadrupole parity.} \end{cases} \tag{4.4}$$

On using 20 grid points in r, we obtained the value of $R = 30.56$ for the dipole symmetry. Their result of $C = 652$ leads, however, to $R = 28.5$. To resolve this discrepancy, we repeated their calculation using their method, and obtained the value, R, for $N = 1$ and $M = \infty$ shown in table 3; this is clearly in good agreement with the results of the grid point calculation.

TABLE 3. EIGENVALUES FOR THE STEENBECK–KRAUSE MODEL

The entries in brackets give the oscillation frequency, Ω, of the field.

$\alpha_0\omega_0' > 0$		$\alpha_0\omega_0' < 0$		truncation level	
dipole	quadrupole	quadrupole	dipole	N	M
30.56 (0)	none	35.36 (0)	none	1	20
30.55 (0)	none	35.37 (0)	none	1	40
30.5463 (0)	none	35.3753 (0)	none	1	∞
56.05 (18.41)	90.08 (53.19)	56.64 (22.43)	84.76 (49.69)	2	20
56.02 (18.40)	90.07 (53.21)	56.66 (22.46)	84.73 (49.73)	2	30
55.9902 (18.3896)	90.0629 (53.2276)	56.6550 (22.4865)	84.7191 (49.7601)	2	∞
62.59 (0)	70.47 (47.49)	68.75 (48.28)	68.44 (46.69)	3	20
82.39 (68.06)	74.95 (54.78)	81.59 (68.08)	73.66 (54.12)	4	20
82.39 (68.05)	74.93 (54.79)	81.59 (68.17)	73.67 (54.18)	4	30
89.51 (71.10)	76.31 (55.36)	87.03 (68.80)	74.56 (54.22)	5	20
87.03 (68.61)	76.08 (55.14)	85.27 (67.33)	74.38 (54.06)	6	20
87.13 (68.76)	76.08 (55.15)	85.36 (67.45)	74.39 (54.07)	7	20
87.13 (68.75)	76.08 (55.15)	85.36 (67.44)	74.39 (54.07)	8	20

We also repeated Steenbeck & Krause's calculation for the quadrupole eigenvalue at the $N = 1$ truncation level, obtaining a value $C = 500.56$, which is in excellent accord with the results of the grid point method, as well as to their value.

Table 3 records the results obtained for various truncation levels and mesh sizes. It is at once apparent that, unlike the case of the α^2 dynamos examined in § 3, the results obtained at the $N = 1$ truncation level are *even qualitatively* misleading. These indicate that, if $\alpha_0\omega_0' > 0$, the only possible solution is of d.c. dipole type; while, if $\alpha_0\omega_0' < 0$, the only possible solution is of d.c. quadrupole type. It may be seen from the table, however, that our results show that solutions of both dipole and quadrupole type exist for either sign of $\alpha_0\omega_0'$. Moreover, it appears that the field most readily excited when $\alpha_0\omega_0' > 0$ is of a.c. quadrupole type while, if $\alpha_0\omega_0' < 0$ it is of a.c. dipole type. As for the α^2 dynamos, however, the fields of dipole and quadrupole type can be excited with almost equal ease, and this distinction is possibly not significant for the model shown. It was clear from supplementary calculations that, if d.c. dynamos exist, they must have critical Reynolds numbers significantly greater than those shown for the a.c. dynamos.

These results seemed at first so surprising that an independent calculation was undertaken in which the solutions at the $N = 2$ level were obtained by a series expansion method which is the natural extension of the one used by Steenbeck & Krause. The results are also reported in table 3 (see the $N = 2$, $M = \infty$ entries), and can be seen to be in good agreement with those of

the grid point calculations. A supplementary point made clear by table 3 is the (computationally unpleasant) fact that N must be at least 4 before qualitatively correct results are obtained (note the $N = 3$ dipole type solutions for $\alpha\omega_0' > 0$). The behaviour of the largest growth rate as a function of $R_\alpha R_\omega$ is shown for both dipole and quadrupole families in figure 1.

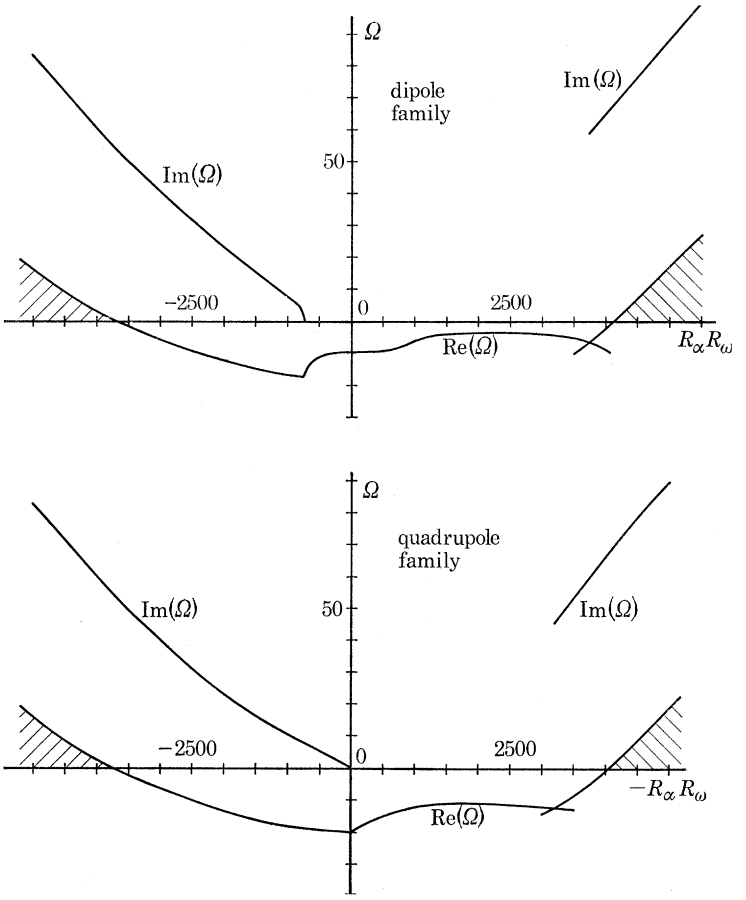

FIGURE 1. The growth rate, $\mathrm{Re}(\Omega)$, of the most easily excited mode as a function of $R_\alpha R_\omega$ in the case of the $\alpha\omega$ dynamo model of Steenbeck & Krause, defined by (4.3). When this mode is oscillatory, the frequency $\mathrm{Im}(\Omega)$ is also shown. For values of $R_\alpha R_\omega$ beneath the shaded regions, the dynamo is self-excited. The truncation level is 16 harmonics and 20 grid points.

The general conclusions arrived at by the study of model 1 were confirmed in calculations performed for two other models. These were

$$\text{model 2:} \quad \left.\begin{aligned} \alpha &= \tfrac{729}{16}\alpha_0 r^8(1-r^2)^2\cos\theta, \\ \omega &= -\tfrac{196833}{40960}\omega_0'(1-r^2)^5, \end{aligned}\right\} \tag{4.5}$$

$$\text{model 3:} \quad \left.\begin{aligned} \alpha &= 24\sqrt{3}\,\alpha_0 r^2(1-r)^2\cos\theta\sin^2\theta; \\ \omega &= -\tfrac{3}{8}\sqrt{3}\,\omega_0'(1-r^2)^2. \end{aligned}\right\} \tag{4.6}$$

As before, the constants were so chosen that the maximum values of α and ω' in the sphere are α_0 and ω_0' respectively. Results are shown in table 4.

It was suggested by Steenbeck & Krause (1966, § 7; 1969*a*, § C) that an $\alpha\omega$ dynamo would function efficiently (i.e. possesses a small R) only if the regions of greatest shear were separated

from those of maximum α effect, and might not function at all if this were not the case. These regions were deliberately separated in model 2, the maximum α occurring at $r = 0.816$, and that of ω' at $r = 0.333$. It is clear that, although the oscillation frequency for this model is indeed smaller, corresponding to the greater 'skin depth' the field must penetrate in spreading from one centre of inductive action to the other (Steenbeck & Krause 1969*a*, § C), there is no evidence that the dynamo is significantly easier to excite. It is interesting to observe, however, that it now seems to be noticeably easier to generate a dipole (quadrupole) type solution when $\alpha_0 \omega_0' < 0$ (> 0) than a quadrupole (dipole) type field. It is nevertheless slightly surprising that Steenbeck & Krause (1969*a*, § F. 1) should report quadrupole eigenvalues so greatly in excess of the dipole eigenvalues for their models.

TABLE 4

The entries in brackets give the oscillation frequency, Ω, of the field.

model no.	defining equation	sign of $\alpha_0 \omega_0'$	dipole eigenvalue	quadrupole eigenvalue	truncation N	truncation M
1	4.3	+	87.1 (68.8)	76.1 (55.1)	8	20
		−	74.4 (54.1)	85.4 (67.4)	8	20
2	4.5	+	257.0 (66.4)	212.0 (49.7)	6–9	20
		−	206.0 (47.4)	254.0 (64.4)	6–9	20
3	4.6	+	113.0 (93.5)	94.8 (77.6)	5	20
		−	94.8 (77.3)	113.0 (93.3)	5	20

TABLE 5. SHELL MODEL

Number of grid points, M, is 20. The entries in brackets give the oscillation frequency, Ω, of the field.

ratio of shell radii, f	$\alpha_0 \omega_0' > 0$		$\alpha_0 \omega_0' < 0$		truncation level, N
	dipole	quadrupole	quadrupole	dipole	
0	87.13 (68.75)	76.08 (55.14)	85.36 (67.44)	74.39 (54.07)	9
0.3	87.30 (69.35)	78.60 (58.70)	85.52 (68.02)	76.82 (57.52)	8
0.4	89.88 (73.65)	84.12 (66.02)	87.97 (72.13)	82.19 (64.63)	8
0.5	98.46 (86.15)	95.74 (81.66)	96.36 (84.33)	93.59 (79.93)	8
0.6	118.4 (114.9)	117.9 (113.4)	116.1 (112.8)	115.5 (111.2)	8
0.65	135.8 (141.2)	135.9 (140.7)	133.4 (138.9)	133.4 (138.3)	8
0.7	160.6 (179.9)	162.9 (183.3)	158.2 (177.7)	159.9 (180.2)	8
0.75	199.1 (230.0)	206.2 (275.7)	196.2 (229.5)	210.8 (243.3)	8
0.75	199.6 (246.6)	203.0 (251.8)	197.1 (244.6)	199.9 (248.4)	9

Some support for Steenbeck & Krause's ideas on the separation of the regions of potent α and ω' was obtained from integrations performed for model 1 in the shell $f \leqslant r \leqslant 1$, rather than the full sphere (table 5). It was supposed that both T and S vanish on $r = f$. This boundary condition is not strictly correct (see § 2) but, for a rapidly oscillating field such as that considered here, there should be little error: the scalars S and T are essentially zero at $r = f - \delta$, where δ is the skin depth corresponding to the oscillation frequency, and the error introduced by supposing them to vanish on $r = f$ instead is probably small.

The evolution of the field with time during a cycle is of some interest. In figures 2 to 5, four half cycles are shown for model 2 at phases of (*a*) 0, (*b*) $\frac{1}{8}\pi$, (*c*) $\frac{1}{4}\pi$, (*d*) $\frac{3}{8}\pi$, (*e*) $\frac{1}{2}\pi$, (*f*) $\frac{5}{8}\pi$, (*g*) $\frac{3}{4}\pi$, and (*h*) $\frac{7}{8}\pi$; the zero of phase is arbitrary. Figures 2 and 3 show dipole and quadrupole oscillations for $\alpha\omega' > 0$; it is clear that the centres of activity migrate from equator to poles. For example, consider the dipole solution shown in figure 2. At each epoch two or three foci of toroidal field

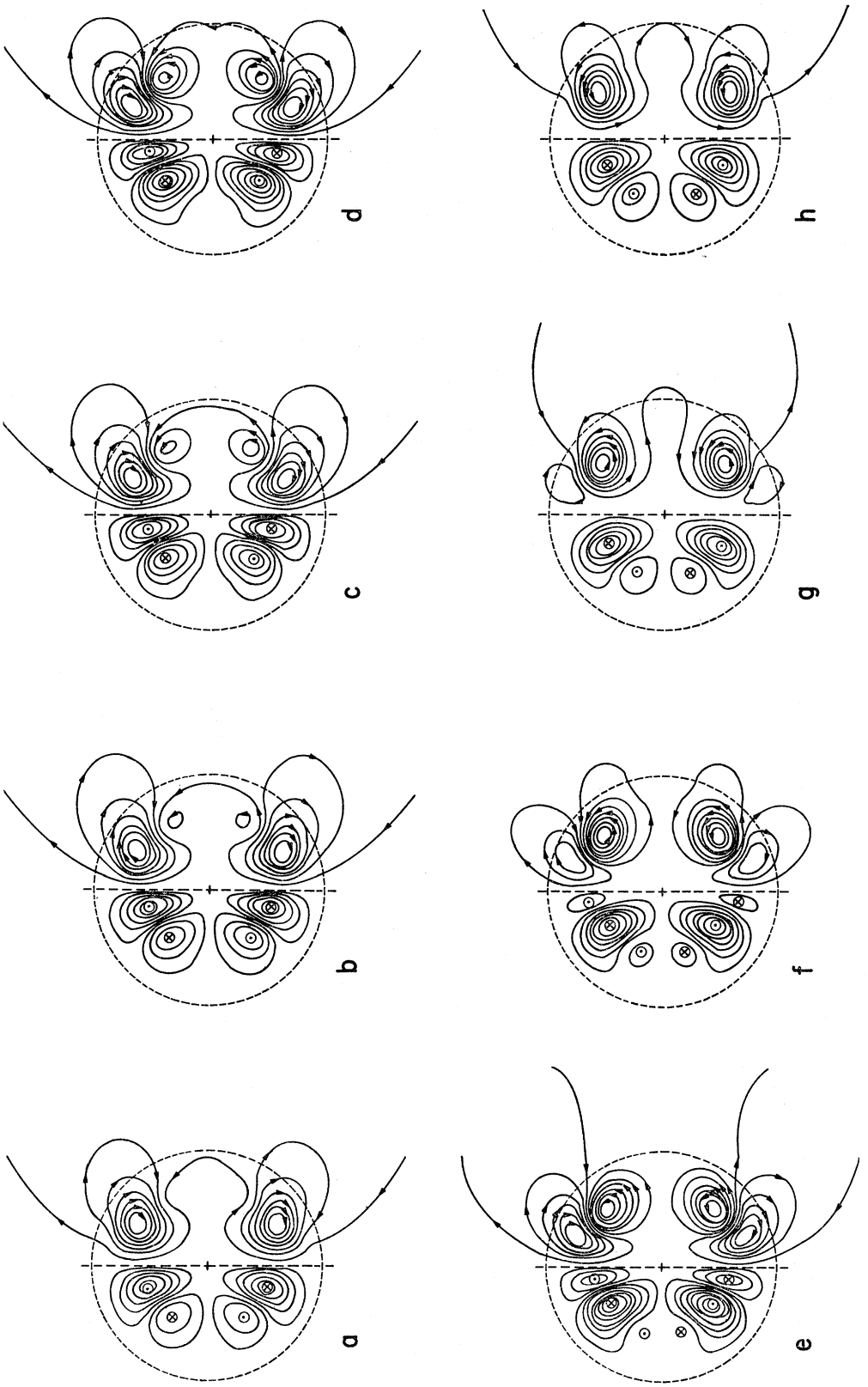

FIGURE 2. The evolution of the marginal dipole oscillation of the $\alpha\omega$ dynamo defined by (4.5) in the case $\alpha_0\omega_0' > 0$. A half cycle is given, and (*a*) shows the field at the (arbitrarily chosen) instant $t = 0$. The values of t of figures (*b*) to (*h*) are then, respectively, $\pi/8\Omega$, $\pi/4\Omega$, $3\pi/8\Omega$, $\pi/2\Omega$, $5\pi/8\Omega$, $3\pi/4\Omega$ and $7\pi/8\Omega$, where Ω is the oscillation frequency, here 66.45 in dimensionless units. Meridian sections are shown, the symmetry axis being dotted. On the right of this axis, the lines of poloidal force are drawn, while on the left lines of constant toroidal field strength are shown, the field being out of the plane of the paper in regions indicated by the encircled dots and into the plane of the paper in regions indicated by the encircled crosses. All contour lines are drawn at equal spacing (in field strength on the left and poloidal stream function on the right). The progression of the pattern, from equator to poles as time increases, is evident. The truncation level is 10 harmonics and 20 grid points, and $R = 257.4$.

PHILOSOPHICAL TRANSACTIONS OF THE ROYAL SOCIETY A MATHEMATICAL, PHYSICAL & ENGINEERING SCIENCES

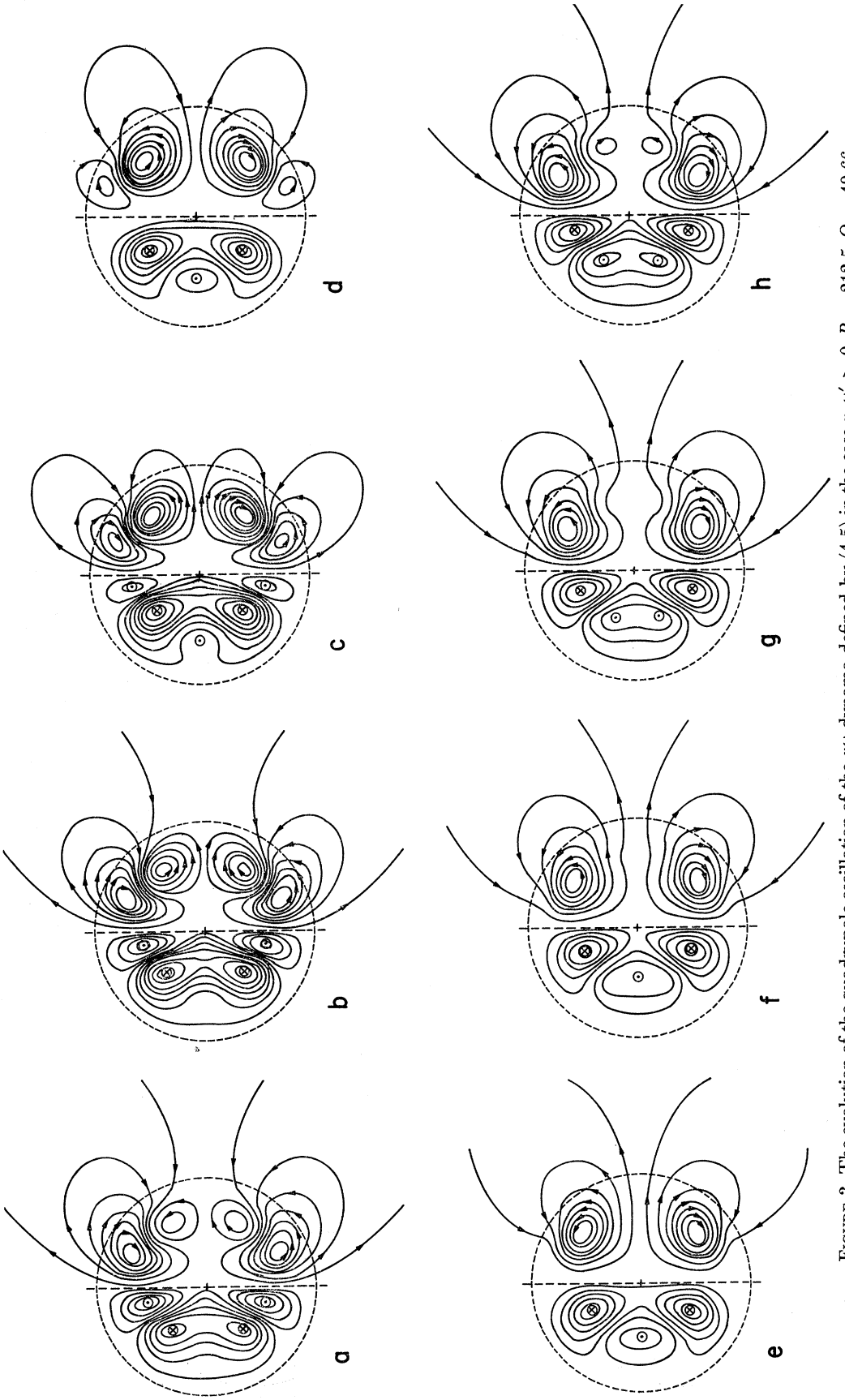

FIGURE 3. The evolution of the quadrupole oscillation of the $\alpha\omega$ dynamo defined by (4.5) in the case $\alpha_0\omega_0' > 0$. $R = 212.5, \Omega = 49.66$. The wave motion is from equator to poles. See also the description of figure 2.

PHILOSOPHICAL TRANSACTIONS OF THE ROYAL SOCIETY A MATHEMATICAL, PHYSICAL & ENGINEERING SCIENCES

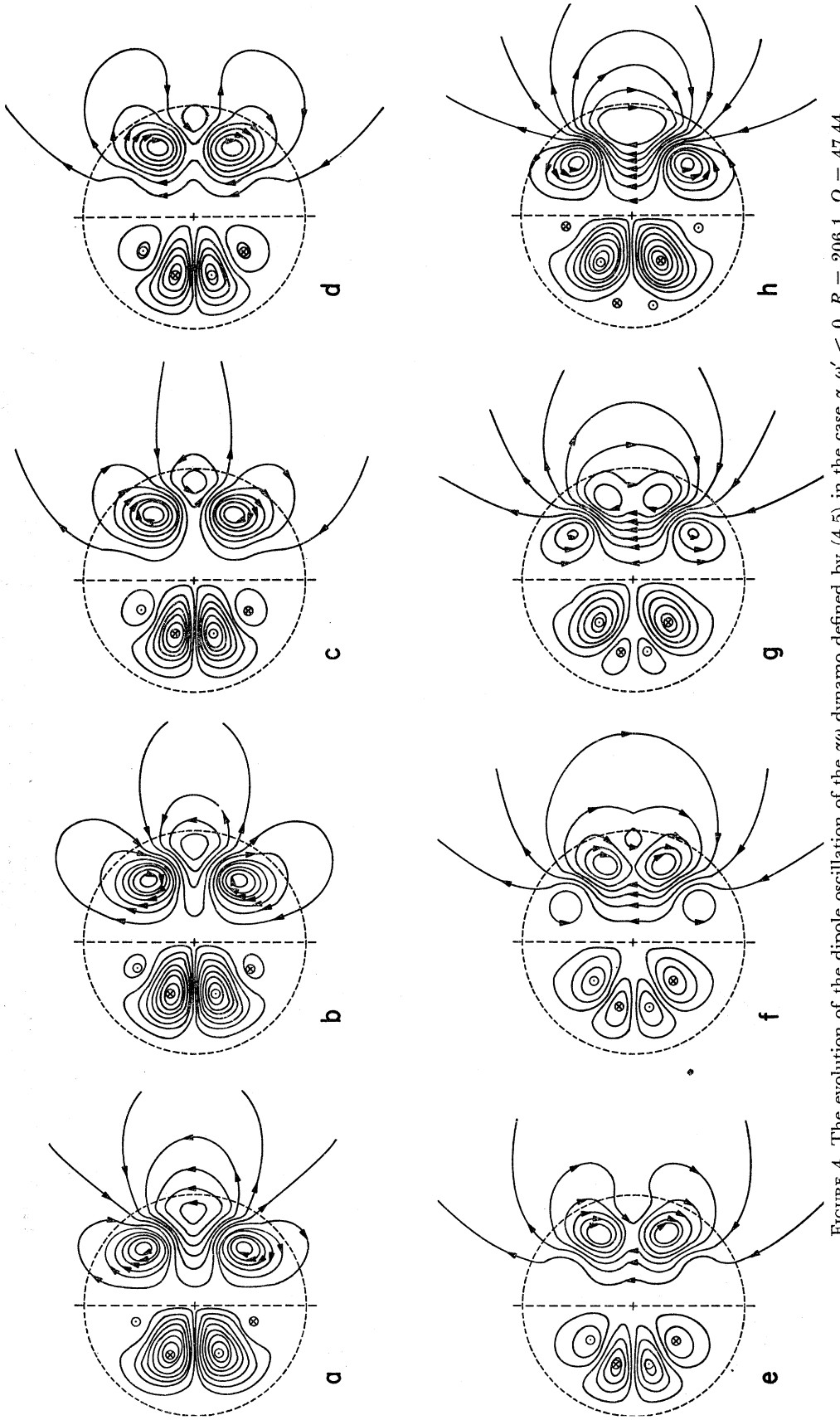

FIGURE 4. The evolution of the dipole oscillation of the $\alpha\omega$ dynamo defined by (4.5) in the case $\alpha_0\omega_0' < 0$. $R = 206.1$, $\Omega = 47.44$. The wave motion is from poles to equator. See also the description of figure 2.

PHILOSOPHICAL TRANSACTIONS OF THE ROYAL SOCIETY A MATHEMATICAL, PHYSICAL & ENGINEERING SCIENCES

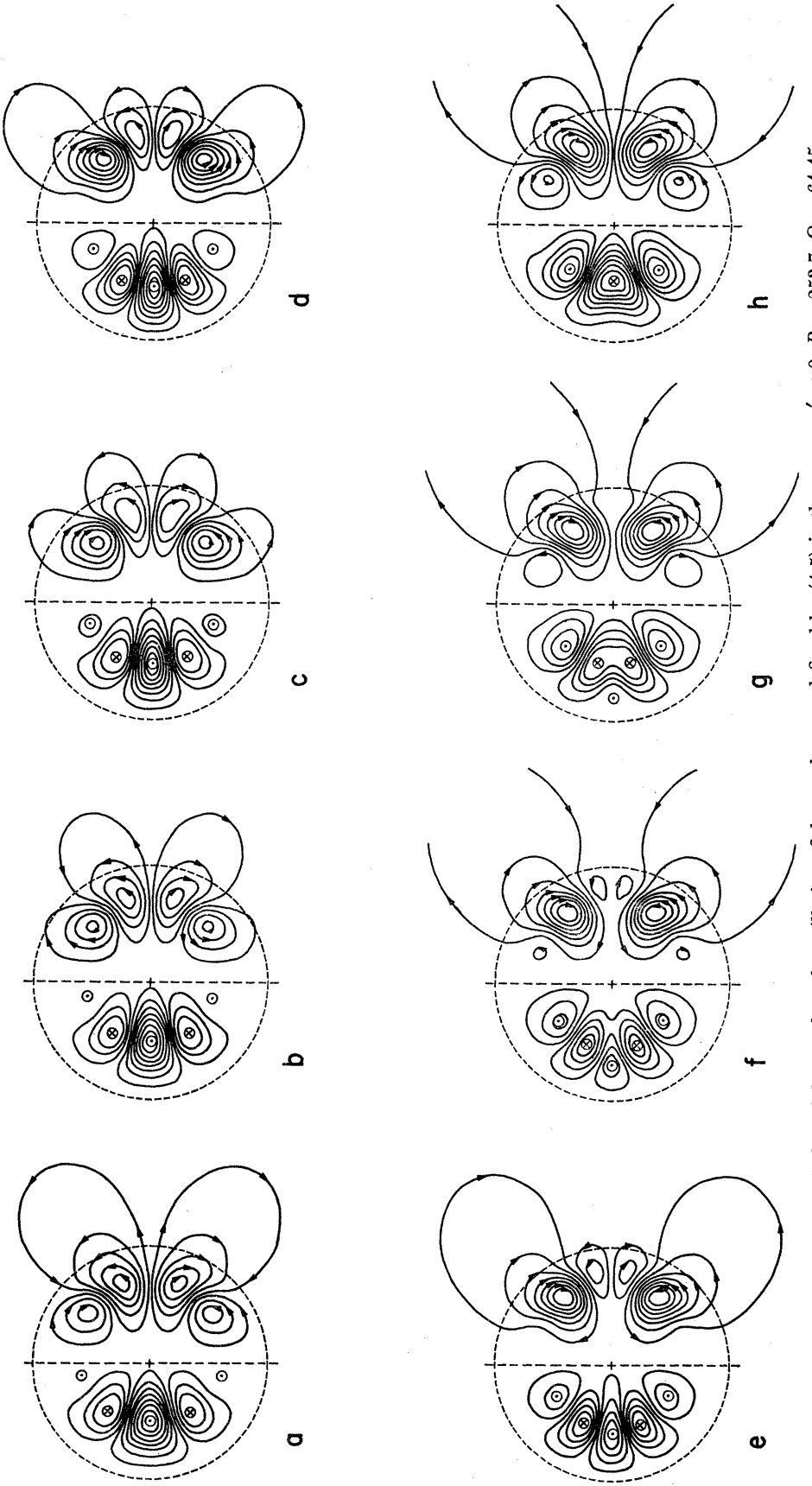

FIGURE 5. The evolution of the quadrupole oscillation of the $\alpha\omega$ dynamo defined by (4.5) in the case $\alpha_0\omega_0' < 0$. $R = 253.7$, $\Omega = 64.45$. The wave motion is from poles to equator. See also the description of figure 2.

can be discerned in each hemisphere. Initially (*a*) there are two, and the one nearer the equator strengthens, expands itself and, in so doing, compresses the focus near the pole, which ultimately starts to weaken. As the equatorward focus expands, the field diminishes near the equatorial plane, and a new focus appears (*e*). This grows, as the focus near the pole withers, until, by the end of the half cycle, it has replaced the original equatorward focus which, however, has now displaced the original focus near the pole. The half cycle is then repeated with all fields of the opposite sign. The sense of migration is reversed for the case of negative $\alpha\omega'$, as figures 4 and 5 illustrate. This is the direction in which sunspots move (cf. Maunder's butterfly diagram).

As Roberts (1967*b*) observed, the oscillatory nature of $\alpha\omega$ dynamos may be anticipated, and understood, from the adaptation to spherical geometry of the planar dynamo waves discovered by Parker (1955). Consider a primary flow in the z direction which is sheared in the y direction. This can generate, from a (poloidal) field in xy planes, a (toroidal) field in the z direction. The α effect can then create, from this toroidal field, currents in the z direction which can support the original poloidal field. Parker showed that the steady self-regenerating field pattern which could be so created would drift steadily in the y direction with a velocity of order ηk, in dimensional units, where k is the wavenumber of the pattern in the y direction. Taking (x, y, z) to correspond to $(\pi-\theta, r, \phi)$, we see that the magnetic field pattern for $\alpha\omega$ dynamos should move along lines of longitude. Moreover, it is easily shown that the sense is that described above: from equator to pole for $\alpha\omega' > 0$, and the reverse for $\alpha\omega' < 0$. The speed of drift is not in good agreement with the Cartesian value, perhaps because poles and equatorial plane here play the roles of absorbing walls (see Parker 1971*a*, *b*, *c*).

In the next section, we will suppress the constants α_0 and ω_0' so far used in the specification of our models. This is permissible because $R_\omega \gg R_\alpha$ and the $(A_\alpha S_\beta T_\gamma)$ interaction is ignored. In fact, α_0 and ω_0' are eliminated by the transformation

$$\left.\begin{aligned} A_\alpha &= \pm\alpha_0 \tilde{A}_\alpha, \quad t_\alpha = \omega_0' \tilde{t}_\alpha, \quad s_\alpha = (\pm\alpha_0\omega_0')^{\frac{1}{2}} \tilde{s}_\alpha, \\ T_\gamma &= \tilde{T}_\gamma, \quad S_\gamma = \tilde{S}_\gamma(\pm\alpha_0/\omega_0')^{\frac{1}{2}}, \quad R = (\pm\alpha_0\omega_0')^{-\frac{1}{2}}\tilde{R}, \end{aligned}\right\} \tag{4.7}$$

which leaves (2.10) and (2.11) unaltered. (The $\pm$ sign is selected in the way necessary to make the radicals real.) The Braginskiĭ theory provides a good example of the use of this transformation. In his expansion scheme, $\alpha_0 = O(\omega_0'/R)$ where $R \gg 1$, but the simple scaling (4.7) transforms all variables to the same order of magnitude.

Calculations on dynamos of $\alpha\omega$ type are more time consuming than for the α^2 dynamos of § 2. This may be attributed in part to the high truncation level required and to the fact that a complex growth rate has to be determined.

5. The effect of meridional circulation on the $\alpha\omega$ dynamos

Partly as a check on the accuracy of the program, the first model considered was identical to one examined by Braginskiĭ (1964*b*). It is defined by

$$\left.\begin{aligned} t(r) &= -r^2(1-r^2)^2 P_1(\cos\theta), \\ s(r) &= 10mr^6(1-r)^2 P_2(\cos\theta), \\ \alpha(r) &= \tfrac{96}{5} r^2(1-r)^2[P_1(\cos\theta) - P_3(\cos\theta)], \end{aligned}\right\} \tag{5.1}$$

[cf. Braginskiĭ 1964*b*, eqns (2.1), (2.2), (2.4), (2.6) and (2.10); the m of (5.1) is Braginskiĭ's η, and the Reynolds number we will seek is Braginskiĭ's β]. Table 6 gives the eigenvalues for R obtained

for the dipole type solution, and also illustrates the convergence of these solutions as the truncation level is increased. The agreement with Braginskiĭ's results, some of which are also listed, is gratifying. Our results were, however, at variance with Braginskiĭ's findings in one respect. Braginskiĭ obtained solutions only for $-0.52 \leqslant m \leqslant -0.12$, and conjectured that only oscillatory solutions existed outside this range. We did, indeed, find only unsteady solutions for $-0.12 < m < 0.14$ but, for all other values of m that we examined, we found that steady fields were the most easily excited. It seems clear, however, that Braginskiĭ succeeded in isolating the range of m in which dynamo action, either steady or unsteady, is most efficient.

TABLE 6. THE REYNOLDS NUMBER, R, FOR STEADY DIPOLE TYPE SOLUTIONS FOR (5.1) FOR $\alpha\omega' > 0$ AS A FUNCTION OF THE STRENGTH, m, OF THE MERIDIONAL CIRCULATION

M is the number of grid points, and N the number of harmonic pairs.

	$M = 20$						$M = 30$	Braginskiĭ results,
m	$N = 4$	$N = 5$	$N = 6$	$N = 7$	$N = 8$	$N = 9$	$N = 4$	$N = 4$
−2.00	96.71	66.62	87.45	77.08	85.72	82.25	—	—
−1.75	81.55	63.30	76.45	71.38	76.39	74.72	—	—
−1.50	67.74	59.40	66.83	64.94	67.27	66.65	—	—
−1.25	57.13	54.56	57.98	57.55	58.29	58.14	—	—
−1.00	48.55	48.29	49.34	49.31	49.42	49.40	48.66	—
−0.75	40.54	40.58	40.72	40.72	40.72	40.72	40.64	—
−0.50	33.56	33.56	33.56	33.56	33.56	33.56	33.63	33.67
−0.40	31.99	31.99	31.99	31.99	31.99	31.99	32.05	32.08
−0.30	31.56	31.56	31.56	31.56	31.56	31.56	31.61	—
−0.20	32.68	32.68	32.68	32.68	32.68	32.68	32.92	—
−0.15	35.04	35.04	35.04	35.04	35.04	35.04	35.12	35.18
0.15	—	130.6	172.0	172.8	172.2	172.3	192.1	—
0.20	112.5	104.0	104.3	104.9	104.8	104.8	—	—
0.30	76.18	73.29	73.48	73.52	73.51	73.51	78.42	—
0.40	67.91	65.67	66.01	65.98	65.98	65.98	—	—
0.50	65.42	63.14	63.65	63.58	63.59	63.59	67.69	—
0.75	66.36	62.57	64.07	63.72	63.80	63.79	69.31	—
1.00	70.62	63.24	67.32	66.16	66.54	66.44	74.27	—
1.25	75.43	62.88	71.55	68.70	69.92	69.53	—	—
1.50	79.90	61.45	76.20	70.80	73.72	72.62	—	—
1.75	83.91	59.39	80.89	72.29	78.03	75.69	—	—
2.00	87.49	57.06	85.32	73.17	82.86	78.78	—	—

We also sought solutions of quadrupole type. These were found to be less readily excited in all cases for which a steady dipole type solution existed. For small values of $|m|$, however, for which the dipole type solution is unsteady, the quadrupole type field, then also oscillatory, was found to be more easily excited. This is consistent with the general conclusions of § 4.

Other types of solutions were also sought. We reversed the sign of t_1 in (5.1) to define a new situation which we refer to as a case of negative $\alpha\omega'$, in contrast to that defined in (5.1) above, for which $\alpha\, \mathrm{d}\omega/\mathrm{d}r$ is positive everywhere *in the northern hemisphere*. Again solutions of both dipole and quadrupole type exist, and the results reported above are repeated (almost identically), with the words quadrupole and dipole interchanged, and the sign of m reversed. For example the most efficient dynamo is now one of quadrupole type, for a value of m near 0.36, the value of R being near 32.0. [In contrast, for the $\alpha\omega' > 0$ case considered earlier, the smallest value of $R(\approx 31.0)$ was for a dipole solution of $m \approx -0.32$.] Fields of dipole form were found to be less readily excited in all cases for which a steady quadrupole type solution existed. For small values of $|m|$, however,

for which the quadrupole type solution is unsteady, the dipole type field, then also oscillatory, was found to be the more easily excited. The eigenvalues for the steady quadrupole type fields are given in table 7. A variety of fields are drawn in figure 6.

TABLE 7. THE REYNOLDS NUMBER, R, FOR STEADY QUADRUPOLE TYPE SOLUTIONS FOR (5.1) IN THE CASE $\alpha\omega' < 0$ AS A FUNCTION OF THE STRENGTH, m, OF THE MERIDIONAL CIRCULATION

20 grid points, 18 harmonics.

m	−1.50	−1.00	−0.75	−0.50	−0.40	−0.30	−0.25
R	88.69	77.09	71.41	70.90	75.22	87.40	101.1
m	0.15	0.20	0.30	0.40	0.50	0.75	1.00
R	39.01	34.82	32.28	32.12	33.30	40.41	50.19

Oscillatory solutions for small $|m|$ have the Reynolds numbers shown in table 8. For the reasons stated in § 2, the unsteady solutions of large frequency, Ω, are not reliable estimates of the converged solutions ($N\to\infty$, $M\to\infty$). For this reason the values shown for $m > 0.10$ and $\alpha\omega' > 0$, and for $m < -0.10$ and $\alpha\omega' < 0$, are probably considerably in error. Their accuracy may, however,

TABLE 8. THE REYNOLDS NUMBER, R, AND OSCILLATION FREQUENCY, Ω, OF UNSTEADY SOLUTIONS FOR (5.1) AS FUNCTIONS OF THE STRENGTH, m, OF MERIDIONAL CIRCULATION

20 grid points. Where there are two lines corresponding to one value of m, the upper is for $N = 4$ and the lower for $N = 5$; otherwise the results are for $N = 5$.

	$\alpha\omega' > 0$					$\alpha\omega' < 0$				
	dipole		quadrupole			quadrupole		dipole		
m	R	Ω	R	Ω	m	R	Ω	R	Ω
−0.20	76.85	38.78	60.72	36.34	0.20	—	—	59.85	35.69
	none found		60.71	36.44		—	—	59.90	35.81
−0.15	71.89	38.65	—	—	0.15	72.53	39.89	—	—
	73.38	39.65	—	—		74.17	41.07	—	—
−0.10	68.55	43.18	59.10	46.94	0.10	68.50	45.72	58.38	46.10
	71.60	47.89	59.63	47.72		71.54	48.40	58.94	46.88
−0.05	69.31	56.04	—	—	0.05	68.93	55.61	—	—
	74.66	63.34	—	—		74.29	62.78	—	—
0.00	74.68	74.60	68.34	72.69	0.00	74.53	74.03	68.28	72.36
	84.59	93.54	71.13	77.57		84.58	93.34	71.11	77.35
0.05	86.66	111.8	—	—	−0.05	86.88	112.2	—	—
	105.8	164.3	93.04	131.1		105.8	164.5	93.20	131.4
0.10	101.5	172.7	102.4	172.9	−0.10	101.6	172.9	102.5	173.1
	166.3	178.7	132.1	277.3		165.9	178.7	132.2	277.8
0.11	132.8	302.0	138.1	308.7	−0.11	132.9	302.6	138.3	309.3
0.12	136.6	327.3	143.8	340.7	−0.12	136.7	327.9	143.9	341.5
0.13	140.1	352.8	149.1	373.3	−0.13	140.3	353.6	149.3	374.2
0.14	143.5	378.5	152.2	406.4	−0.14	143.6	379.5	154.4	407.5
0.15	none found		200.7	305.4	−0.15	—	—	200.4	305.1

possibly be sufficient to indicate that solutions do exist for these values of m, even though they require large values of R, and vary rapidly in space and time. A comparison of the $N = 4$ and $N = 5$ entries elsewhere in the table also suggest that the values of R and Ω obtained for $M = 20$ and $N = 5$ will not be closer to their fully converged values than 10 % of those values.

PHILOSOPHICAL TRANSACTIONS OF THE ROYAL SOCIETY A MATHEMATICAL, PHYSICAL & ENGINEERING SCIENCES

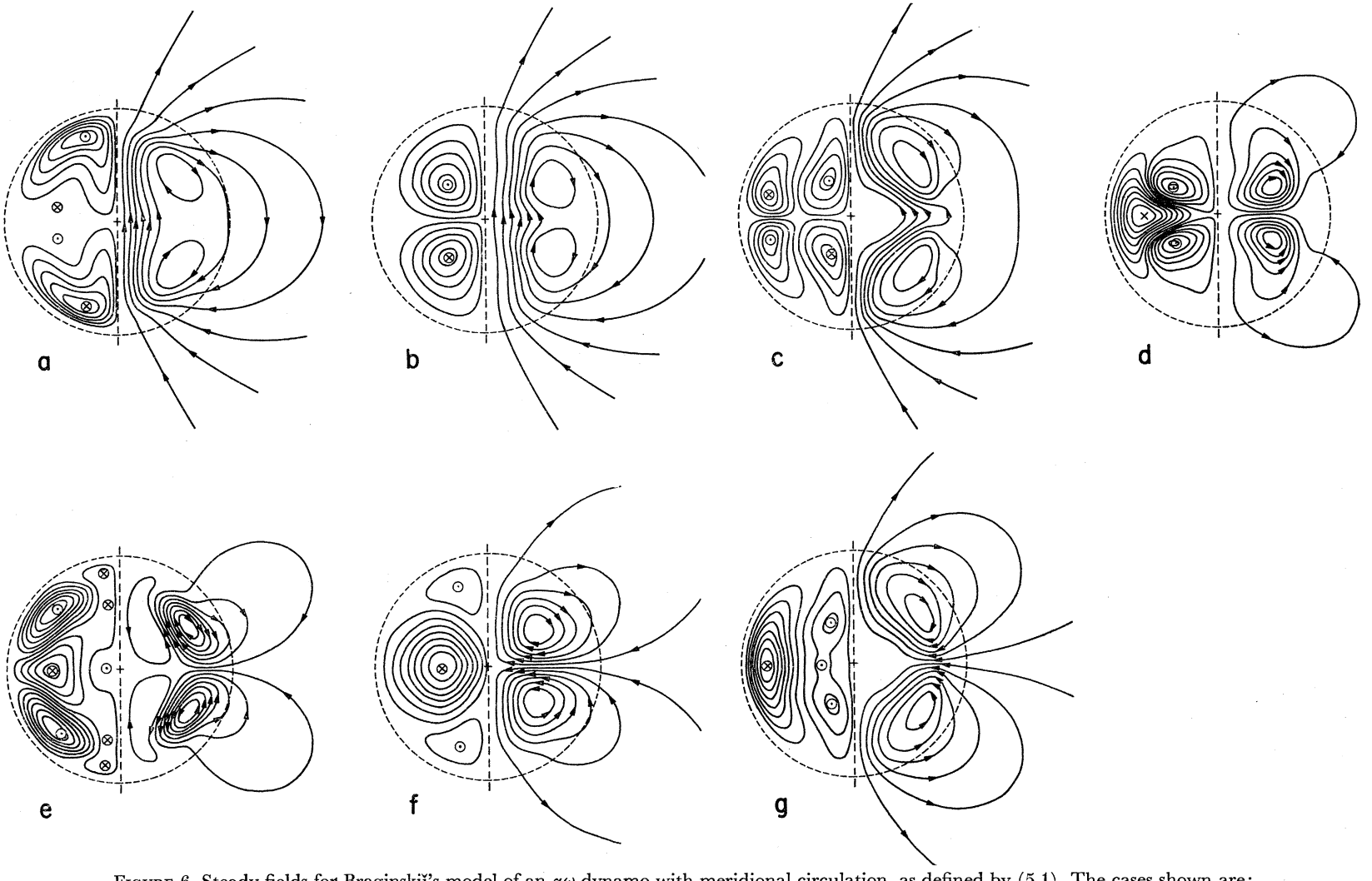

FIGURE 6. Steady fields for Braginskiĭ's model of an $\alpha\omega$ dynamo with meridional circulation, as defined by (5.1). The cases shown are:

(*a*) $\alpha\omega' > 0$, $m = 0.50$, $R = 63.59$, dipole type,
(*b*) $\alpha\omega' > 0$, $m = -0.31$, $R = 31.54$, dipole type,
(*c*) $\alpha\omega' < 0$, $m = -0.55$, $R = 82.39$, dipole type,
(*d*) $\alpha\omega' > 0$, $m = -0.40$, $R = 66.22$, quadrupole type,
(*e*) $\alpha\omega' > 0$, $m = 0.50$, $R = 112.7$, quadrupole type,
(*f*) $\alpha\omega' < 0$, $m = 0.40$, $R = 32.12$, quadrupole type,
(*g*) $\alpha\omega' < 0$, $m = -0.50$, $R = 70.90$, quadrupole type.

Cases (*b*) and (*f*) are associated with a small Reynolds number, and have a particularly simple spatial structure. The truncation level was 16 harmonics and 20 grid points. See also the description of figure 2.

The general behaviour of R as a function of m is shown in figures 7 and 8. To facilitate comparison with other models discussed later, the motions have here been rescaled in the manner permitted by the argument of § 4. Equation (5.1) is replaced by

$$\text{model 1:} \quad \left\{ \begin{aligned} t(r) &= -\frac{3\sqrt{3}}{8} r^2(1-r^2)^2 P_1(\cos\theta), \\ s(r) &= \frac{7168\sqrt{2}}{729} m r^6 (1-r)^2 P_2(\cos\theta), \\ \alpha(r) &= \frac{48\sqrt{3}}{5} r^2(1-r)^2 [P_1(\cos\theta) - P_3(\cos\theta)]. \end{aligned} \right\} \tag{5.2}$$

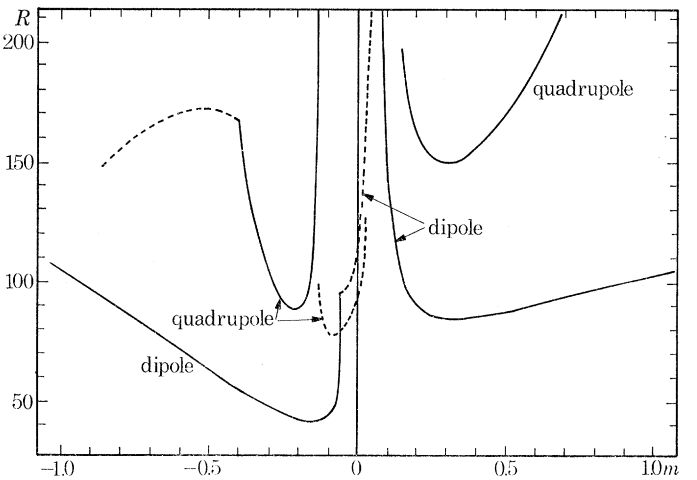

FIGURE 7. The critical Reynolds number, R, as a function of the meridional circulation speed, m, for the Braginskiĭ model, normalized to conform with (5.2). The dashed lines refer to oscillatory modes. The truncation level was 18 harmonics and 20 grid points. It was supposed that $\alpha\omega'$ was positive.

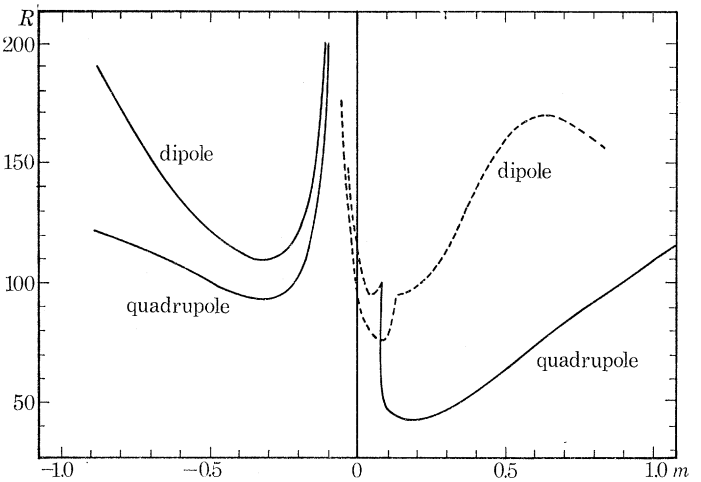

FIGURE 8. The case described in the caption to figure 7, except that $\alpha\omega'$ was assumed to be negative.

The maximum value of the spatial gradient of ω, i.e.

$$\frac{\mathrm{d}\omega}{\mathrm{d}r} = \frac{3\sqrt{3}}{2} r(1-r^2), \tag{5.3}$$

occurs at $r = 1/\sqrt{3}$, and is then unity. Likewise the maximum value of

$$\alpha = 24\sqrt{3}\, r^2(1-r)^2 \cos\theta \sin^2\theta, \tag{5.4}$$

in the northern hemisphere is also unity; it occurs where $r = \frac{1}{2}$ and $\theta = \arccos(1/\sqrt{3})$. These were also the considerations which guided the normalization used in § 4. In addition, we now have a poloidal flow defined by the stream function

$$\psi \equiv -s_2(r)\sin\theta\frac{\mathrm{d}P_2}{\mathrm{d}\theta} = \frac{7168\sqrt{2}}{243}mr^6(1-r)^2\cos\theta\sin^2\theta, \tag{5.5}$$

and this assumes its maximum value of $\psi_{\max} = 7m/16\sqrt{6}$ when $r = 3/4$, $\theta = \arccos(1/\sqrt{3})$. A typical meridional flow speed may be obtained by dividing the flux, $2\pi\psi_{\max}$, of fluid between this circle of latitude and the surface by the area of the collar-shaped surface joining radially this circle to a circle at the same latitude on the surface. In the present case, this area is $7\pi/8\sqrt{6}$, so that the typical meridional flow speed is m. This method of normalizing the meridional flows will also be used, without detailed discussion, in the models considered later in this section.

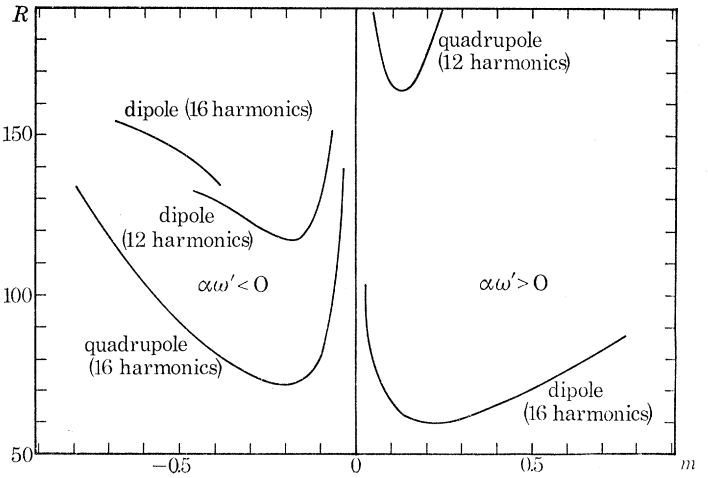

FIGURE 9. The critical Reynolds number, R, as a function of the meridional circulation speed, m, for model 2, defined in (5.6). Only steady solutions are shown. On the right of the axis $m > 0$ and $\alpha\omega' > 0$; on the left $m < 0$ and $\alpha\omega' < 0$. The dynamo was not easily excited for $m < 0$ and $\alpha\omega' > 0$, or for $m > 0$ and $\alpha\omega' < 0$. The truncation level was 20 grid points, and 12 or 16 harmonics as indicated.

An inspection of figures 7 and 8 again shows at once that one sense of meridional circulation greatly facilitates dynamo action while the other inhibits it. Moreover, if the sign of $\alpha\omega'$ is reversed for fixed m, the roles of favourable and unfavourable circulations are reversed.

The next model considered is defined by (cf. equation (4.5))

$$\text{model 2:} \quad \left\{ \begin{aligned} t_1(r) &= -\frac{19683}{40960}r^2(1-r^2)^5, \\ s_2(r) &= \frac{49\sqrt{42}}{144}mr^3(1-r^2)^2, \\ A_1(r) &= \frac{729}{16}r^8(1-r^2)^2. \end{aligned} \right\} \tag{5.6}$$

The constants of proportionality are selected so that $\omega' = \omega'(r)$ and α have unit maxima in the northern hemisphere, while the representative meridional flow, defined as above, is m.

It was found once more that the easiest dynamo to excite was of dipole type of $\alpha\omega' > 0$ and of quadrupole type of $\alpha\omega' < 0$. Now, however, the meridional circulation for which these most favourable solutions are attained is opposite to that of model 1. No convincing results were

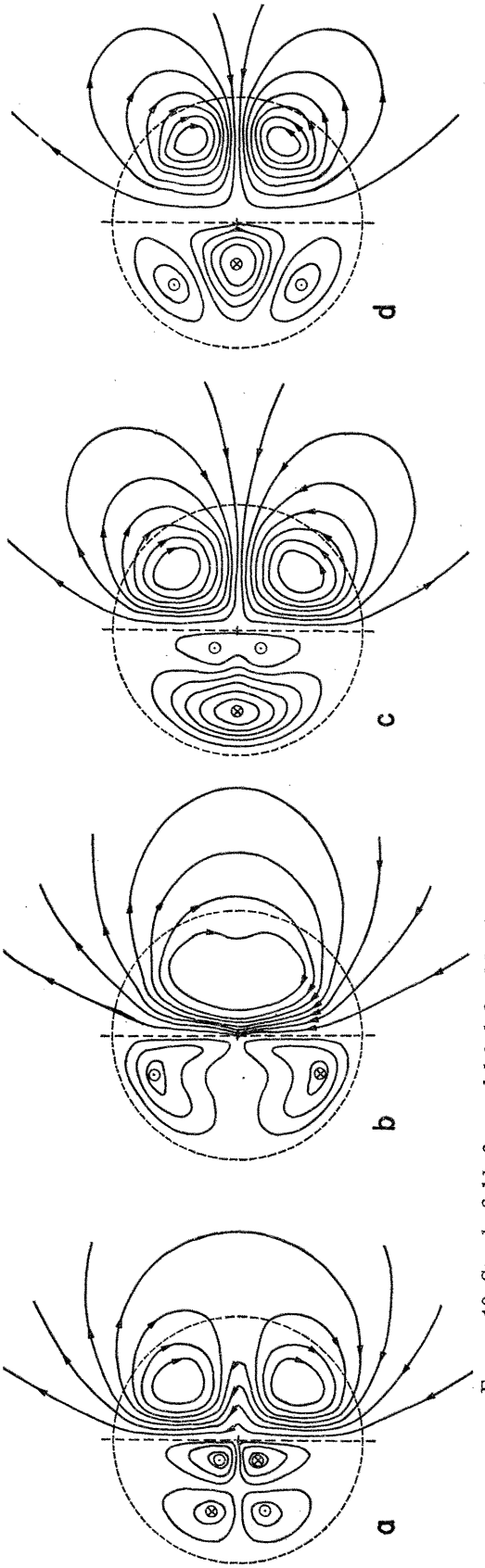

FIGURE 10. Steady fields for model 2 defined by (5.6). The cases shown are:
(*a*) $\alpha\omega' < 0$, $m = -0.159$, $R = 118.2$, dipole type,
(*b*) $\alpha\omega' > 0$, $m = 0.227$, $R = 59.81$, dipole type,
(*c*) $\alpha\omega' < 0$, $m = -0.204$, $R = 71.90$, quadrupole type,
(*d*) $\alpha\omega' > 0$, $m = 0.091$, $R = 168.3$, quadrupole type.
The truncation level was 16 harmonics and 20 grid points. See also description of figure 2.

PHILOSOPHICAL TRANSACTIONS OF THE ROYAL SOCIETY A MATHEMATICAL, PHYSICAL & ENGINEERING SCIENCES

obtained for $\alpha\omega' m < 0$. The Reynolds numbers for steady dynamo action in the cases of positive $\alpha\omega' m$ are shown in figure 9, solutions for $\alpha\omega' > 0$ and $m > 0$ being on the right of the central axis, and those for $\alpha\omega' < 0$ and $m < 0$ on the left. Four field structures are given in figure 10.

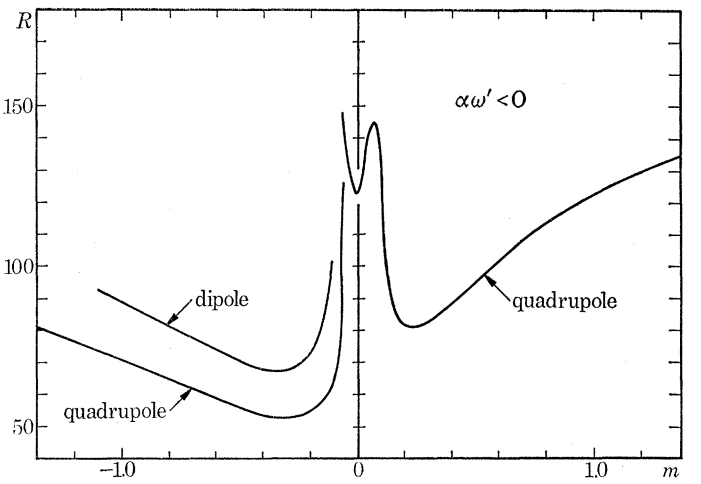

FIGURE 11. The critical Reynolds number, R, as a function of the meridional circulation speed, m, for model 3, defined by (5.7), for the case $\alpha\omega' < 0$. The truncation level was 16 harmonics for the steady solutions, and 8 harmonics for the oscillatory solutions near $m = 0$. In each case, 20 grid points were used. The following results were also obtained for 18 harmonics and 20 grid points: dipole $m = -0.682$, $R = 86.11$; quadrupole $m = -1.02$, $R = 71.68$ and $m = 1.36$, $R = 131.0$. The last two of these results indicate converged values.

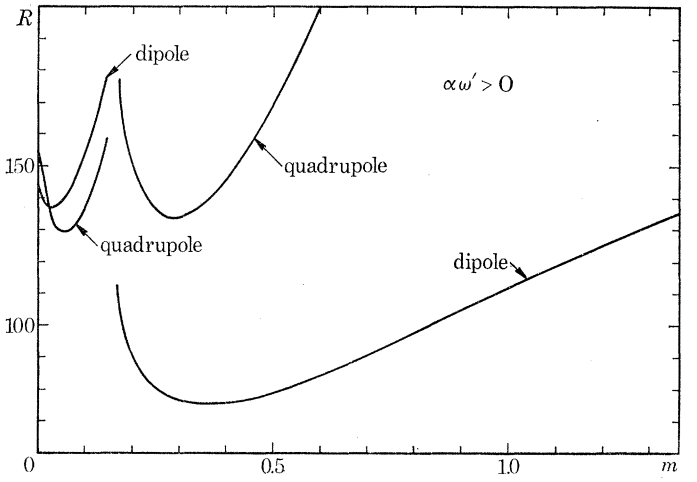

FIGURE 12. The case described in the caption to figure 11 but for $m > 0$ and $\alpha\omega' > 0$. The truncation level was again 16 harmonics and 20 grid points. The following results were also obtained for 18 harmonics and 20 grid points: dipole $m = 1.36$, $R = 150.2$; and $m = 0.273$, $R = 78.16$. Each of these indicate excellent convergence.

The third model examined is defined by

$$\text{model 3:} \quad \left\{ \begin{aligned} t_1(r) &= -6t_3(r) = \tfrac{2}{5}r^4, \\ s_2(r) &= \frac{28\sqrt{2}}{27} m r^3(1-r), \\ A_1(r) &= r. \end{aligned} \right\} \tag{5.7}$$

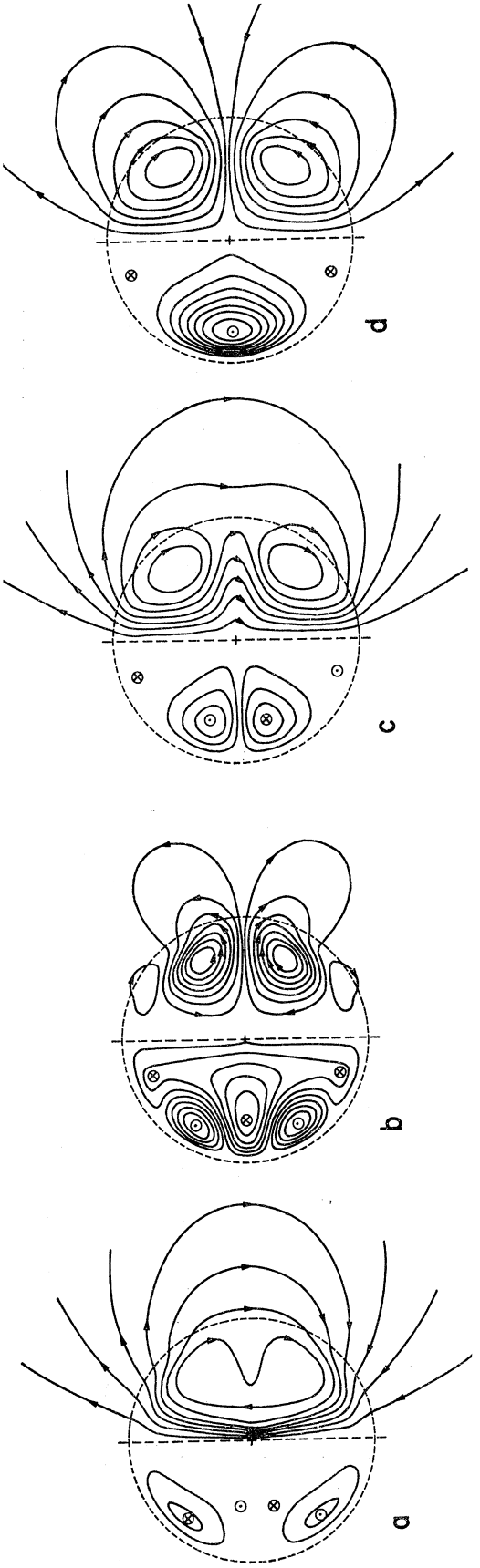

FIGURE 13. Steady fields for model 3 defined by (5.7). The cases shown are:
(*a*) $\alpha\omega' > 0$, $m = 0.341$, $R = 79.87$, dipole type,
(*b*) $\alpha\omega' > 0$, $m = 0.273$, $R = 134.1$, quadrupole type,
(*c*) $\alpha\omega' < 0$, $m = -0.307$, $R = 67.85$, dipole type,
(*d*) $\alpha\omega' < 0$, $m = -0.307$, $R = 53.26$, quadrupole type.
The truncation level was 16 harmonics and 20 grid points. See also the description of figure 2.

PHILOSOPHICAL TRANSACTIONS OF THE ROYAL SOCIETY A MATHEMATICAL, PHYSICAL & ENGINEERING SCIENCES

A particular feature of this model lies in the fact that the angular velocity $\omega(r,\theta)$ is $\frac{1}{2}(r\sin\theta)^2 = \frac{1}{2}\varpi^2$, and is constant on cylindrical surfaces drawn round the axis of the cylinder. It is often found that shearing motion of this type (geostrophic flow) will arise from (say) convective motions in a rapidly rotating system provided the effects of density stratification are not too great. The maximum value of $|\text{grad}\,\omega| = \partial\omega/\partial\varpi = \varpi$ is unity and occurs at the equator.

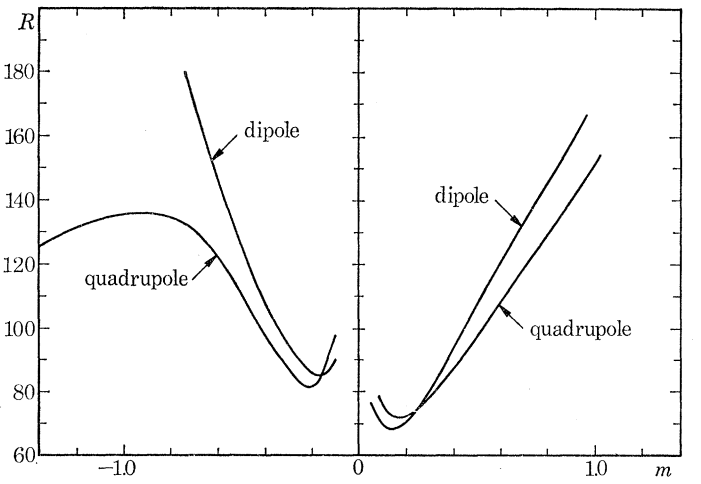

FIGURE 14. The critical Reynolds number, R, as a function of the meridional circulation speed, m, for model 4 defined by (5.8) for the case $\alpha\omega' > 0$. The truncation level was 18 harmonics and 20 grid points. The difference between dipole and quadrupole states is clearly small for a wide range of m.

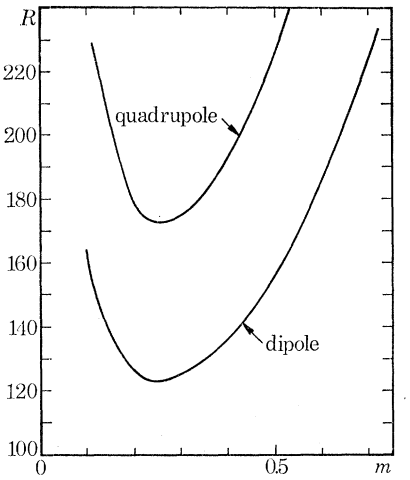

FIGURE 15. The case described in the caption to figure 14 but for $\alpha\omega' < 0$ and $m > 0$. The dynamo was not readily excited for $m < 0$.

Most complete results were obtained in the case $\alpha\omega' < 0$. Like both of the previous models, the quadrupole solutions were easier to excite than the dipole solutions for all values of m apart from those in an extremely small range of oscillatory solutions near $m = 0$. Negative m assist dynamo action, while positive m impede it. The results obtained are shown in figure 11. Solutions were also obtained for positive m in the case $\alpha\omega' > 0$. Here the dipole type solutions were found easier to excite than the quadrupole solutions. The results are shown in figure 12. Some solutions are depicted in figure 13.

In complete contrast with the last case, model 4 was defined by

$$\text{model 4:} \quad \left.\begin{aligned} t_1(r) &= \tfrac{3}{2}t_3(r) = \tfrac{1}{10}r^4, \\ s_2(r) &= \frac{28\sqrt{2}}{27}mr^3(1-r), \\ A_1(r) &= r, \end{aligned}\right\} \tag{5.8}$$

the angular velocity $\omega(r, \theta)$ now being $\frac{1}{2}z^2$, and is constant on planes of constant z. The maximum value of $|\text{grad}\,\omega| = \partial\omega/\partial z = z$ is unity and occurs at the north pole.

Results were most easily obtained in the case $\alpha\omega' > 0$, and are shown in figure 14. Positive m assist dynamo action while negative m impede it. The case $\alpha\omega' < 0$ is illustrated in figure 15. The results do not conform well with the pattern indicated by models 1 to 3. Some fields are drawn in figure 16.

Since, in the ranges of m of major interest, the dipolar dynamos described in this section are steady, one must again wonder, following Weiss (1971), how they evade the restrictions of Cowling's theorem on the equatorial plane, E. Only neutral lines of the poloidal field, $\boldsymbol{B}_p$, can cause difficulties, for elsewhere the electric fields induced by the meridional flow, $\boldsymbol{u}_p$, from $\boldsymbol{B}_p$ can create the required toroidal current. It is easy to convince oneself, however, that one or more neutral lines (encircling the symmetry axis) must exist in the equatorial plane. On these lines $\boldsymbol{u}_p \times \boldsymbol{B}_p$ vanishes, and since α is zero everywhere on E, αB_ϕ must vanish also. There is, then, nothing to maintain j_ϕ. If the neutral line were of O-type, B_ϕ would necessarily vanish to a higher order than j_ϕ, and Cowling's argument would apply. In actual practice, the O-type lines occur in pairs symmetrically situated above and below the equatorial plane. Here Cowling's argument is inapplicable, since the α-effect is operative. The neutral lines on the equatorial plane are of X-type, at which j_ϕ vanishes. In fact, from parity considerations, it must vanish quadratically. To test this numerically we returned to model (5.1), and found that for $N = 2$, 4 and 9 and $M = 40$, 20 and 16, respectively ($R = 31.71$, 31.56 and 31.50, respectively) there were single simple zeros of $\boldsymbol{B}_p$ on the equatorial plane at $\varpi = 0.694$, 0.784 and 0.785 and zeros of j_ϕ at $\varpi = 0.802$, 0.788 and 0.788, respectively. Clearly, as the degree of truncation increases (particularly N), the two zeros approach one another in a sufficiently convincing way to confirm the argument given above.

6. Rädler's dynamos

Rädler (1969*a*) has observed that the statistical properties of turbulence occurring in a rotating fluid will exhibit a preferred direction (namely, that of the rotation axes), and that, in consequence, the mean electromotive force created by the microscale will also depend on that direction. This effect does *not* depend on the existence of other factors (such as gradients in density and/or turbulent intensity) which would create helicity. For clarity, therefore, we will omit the α effect in the following discussion, supposing the turbulence to be without helicity. The resulting e.m.f. is then, in the first approximation, linear in the gradients of $\boldsymbol{B}$, rather than linear in $\boldsymbol{B}$ itself. Following Rädler (1969*a*), we take

$$\mathscr{E}_i \equiv \overline{(\boldsymbol{u}' \times \boldsymbol{B}')}_i = -\beta\epsilon_{ijk}\frac{\partial B_k}{\partial x_j} - \beta_1\omega_j\frac{\partial B_i}{\partial x_j} - \beta_2\omega_j\frac{\partial B_j}{\partial x_i}, \tag{6.1}$$

where $\boldsymbol{\omega}$ is the local vorticity of the mean flow, and β_1 and β_2 are constants (of dimensions L^2) determined by the properties of the turbulence. The turbulent conductivity, σ_T, is related to the

PHILOSOPHICAL TRANSACTIONS OF THE ROYAL SOCIETY A MATHEMATICAL, PHYSICAL & ENGINEERING SCIENCES

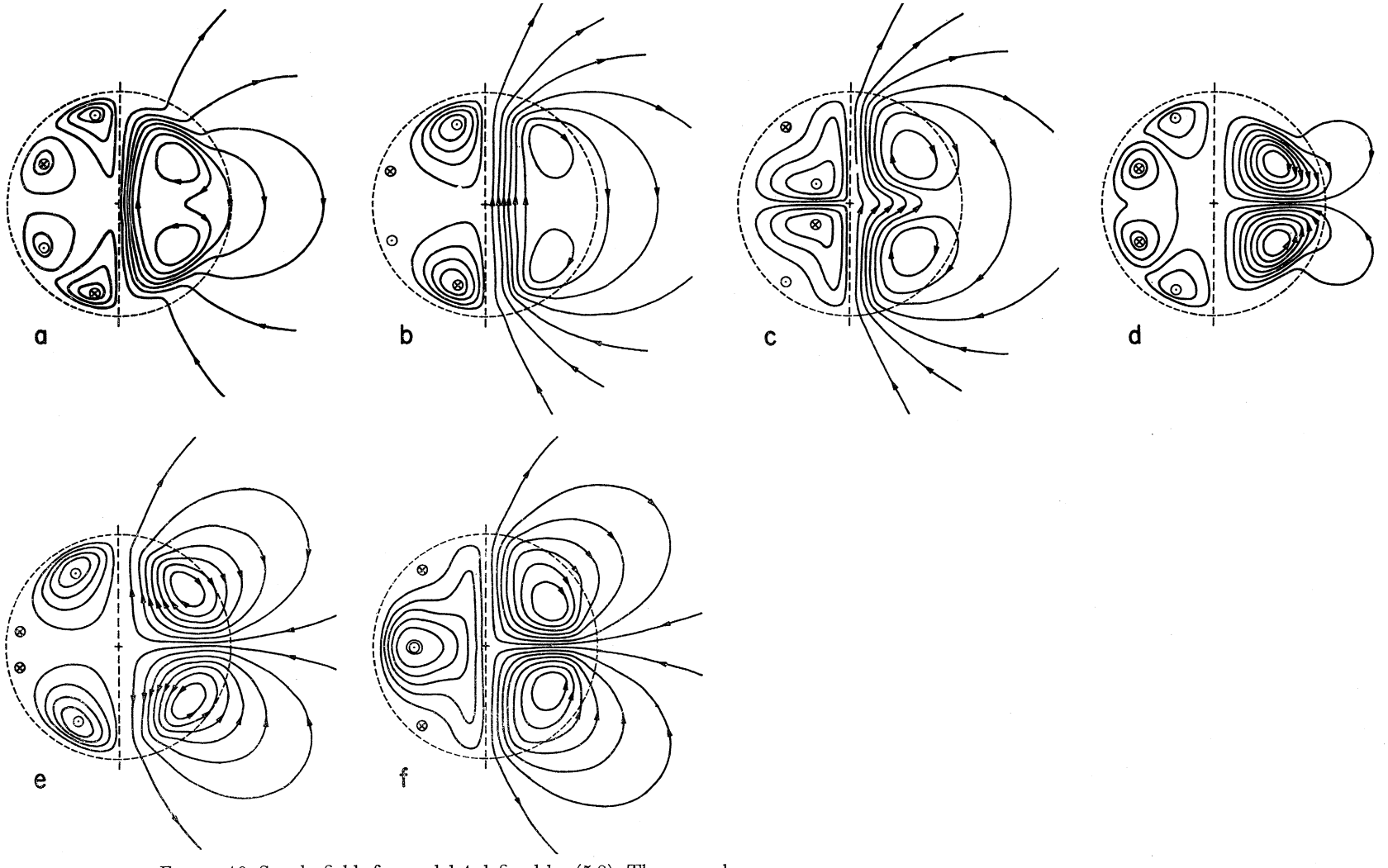

FIGURE 16. Steady fields for model 4 defined by (5.8). The cases shown are:

(*a*) $\alpha\omega' < 0$, $m = 0.273$, $R = 124.3$, dipole type,
(*b*) $\alpha\omega' > 0$, $m = 0.136$, $R = 68.32$, dipole type,
(*c*) $\alpha\omega' > 0$, $m = -0.205$, $R = 86.11$, dipole type,
(*d*) $\alpha\omega' < 0$, $m = 0.273$, $R = 173.1$, quadrupole type,
(*e*) $\alpha\omega' > 0$, $m = 0.205$, $R = 72.23$, quadrupole type,
(*f*) $\alpha\omega' > 0$, $m = -0.239$, $R = 82.51$, quadrupole type.

The truncation level was 18 harmonics and 20 grid points. See also the description of figure 2.

constant β (dimensions L^2/T) and the molecular conductivity, σ, by $\sigma_T = \sigma/(1+\mu\sigma\beta)$. Ohm's law for the mean field becomes

$$\boldsymbol{j} = \sigma_T[\boldsymbol{E}+\boldsymbol{u}\times\boldsymbol{B}-\beta_1\boldsymbol{\omega}\cdot\nabla\boldsymbol{B}-\beta_2(\nabla\boldsymbol{B})\cdot\boldsymbol{\omega}]. \tag{6.2}$$

Clearly, the effectiveness of these new e.m.fs in altering the global fields depends on the magnitudes of the Reynolds numbers,

$$R_\beta = |\omega\beta|/\eta, \tag{6.3}$$

where β now stands for either β_1 or β_2, and $\eta = 1/\mu\sigma_T$.

It is straightforward to include the new electromotive forces in the Bullard & Gellman (1954) formalism. Restricting attention, for simplicity, to the case of axisymmetry, we need only replace the expressions (ATS) and (AST), given by (2.16) and (2.17) in the case of the α-effect, by

$$N_\gamma(A_\alpha T_\beta S_\gamma) = \beta_1 c_\alpha\left[\frac{p_\alpha t_\alpha}{r}\frac{\partial}{\partial r}\left(\frac{T_\beta}{r}\right)-\frac{c_\gamma T_\beta}{r^2}\frac{\partial t_\alpha}{\partial r}\right]G_{\alpha\beta\gamma}+\beta_2\left[(c_\beta p_\beta - c_\alpha c_\gamma)\frac{T_\beta}{r^2}\frac{\partial t_\alpha}{\partial r}-c_\alpha p_\alpha\frac{t_\alpha T_\beta}{r^3}\right]G_{\alpha\beta\gamma}, \tag{6.4}$$

$$\begin{aligned}N_\gamma(A_\alpha S_\beta T_\gamma) = &-\beta_1\left[c_\alpha p_\alpha\frac{\partial}{\partial r}\left\{\frac{t_\alpha}{r}\frac{\partial}{\partial r}\left(\frac{1}{r}\frac{\partial S_\beta}{\partial r}\right)\right\}+c_\beta p_\beta\frac{\partial}{\partial r}\left(\frac{S_\beta}{r^3}\frac{\partial t_\alpha}{\partial r}\right)+\frac{c_\gamma p_\gamma}{r^3}\frac{\partial t_\alpha}{\partial r}\frac{\partial S_\beta}{\partial r}\right.\\&\left.-c_\alpha c_\gamma\frac{\partial}{\partial r}\left(\frac{1}{r^2}\frac{\partial t_\alpha}{\partial r}\frac{\partial S_\beta}{\partial r}\right)-p_\beta c_\gamma p_\gamma\frac{S_\beta}{r^4}\frac{\partial t_\alpha}{\partial r}+p_\alpha p_\beta p_\gamma\frac{t_\alpha}{r^2}\frac{\partial}{\partial r}\left(\frac{S_\beta}{r^2}\right)\right]G_{\alpha\beta\gamma}\\&+\beta_2\left[c_\alpha p_\alpha\frac{\partial}{\partial r}\left(\frac{t_\alpha}{r^3}\frac{\partial S_\beta}{\partial r}\right)-c_\beta p_\beta\frac{\partial}{\partial r}\left(\frac{S_\beta}{r^3}\frac{\partial t_\alpha}{\partial r}\right)+c_\gamma p_\gamma\frac{1}{r}\frac{\partial t_\alpha}{\partial r}\frac{\partial}{\partial r}\left(\frac{1}{r}\frac{\partial S_\beta}{\partial r}\right)\right.\\&\left.+c_\alpha c_\gamma\frac{\partial}{\partial r}\left(\frac{1}{r^2}\frac{\partial t_\alpha}{\partial r}\frac{\partial S_\beta}{\partial r}\right)-c_\alpha p_\alpha p_\beta\frac{\partial}{\partial r}\left(\frac{t_\alpha S_\beta}{r^4}\right)-p_\alpha p_\beta p_\gamma\frac{t_\alpha}{r^2}\frac{\partial}{\partial r}\left(\frac{S_\beta}{r^2}\right)\right]G_{\alpha\beta\gamma}.\end{aligned} \tag{6.5}$$

In deriving these expressions, we have made use of the results, easily established by repeated integration by parts,

$$\int Y_\alpha\frac{\partial Y_\beta}{\partial\theta}\frac{\partial Y_\gamma}{\partial\theta}\,\mathrm{d}\Omega = -c_\alpha G_{\alpha\beta\gamma}, \tag{6.6}$$

$$\int\frac{\partial^2 Y_\alpha}{\partial\theta^2}\frac{\partial Y_\beta}{\partial\theta}\frac{\partial Y_\gamma}{\partial\theta}\,\mathrm{d}\Omega = c_\beta c_\gamma G_{\alpha\beta\gamma}, \tag{6.7}$$

$$\int\frac{\partial Y_\alpha}{\partial\theta}\frac{\partial Y_\beta}{\partial\theta}\frac{\partial Y_\gamma}{\partial\theta}\cos\theta\,\mathrm{d}\Omega = (c_\beta p_\beta - c_\alpha c_\gamma)\,G_{\alpha\beta\gamma}. \tag{6.8}$$

We used expressions (6.4) and (6.5) in the computations which are reported below.

In the particular case $\beta_1 = -\beta_2 = \beta$, (6.2) reduces to the easily appreciated form

$$\boldsymbol{j} = \sigma_T[\boldsymbol{E}+\boldsymbol{u}\times\boldsymbol{B}+\mu\beta\boldsymbol{\omega}\times\boldsymbol{j}]. \tag{6.9}$$

It is evident that the rate at which the new e.m.f. supplies magnetic energy is then proportional to

$$\int\boldsymbol{B}\cdot\mathrm{curl}\,(\beta\boldsymbol{\omega}\times\boldsymbol{j})\,\mathrm{d}V = -\int\beta(\boldsymbol{j}\cdot\boldsymbol{B})\,(\boldsymbol{\omega}\cdot\mathrm{d}\boldsymbol{S}). \tag{6.10}$$

If, for example, $\boldsymbol{\omega}$ is uniform over the boundary (or if β is of opposite sign in opposite hemispheres), the integral on the right vanishes, i.e. the $\boldsymbol{\omega}\times\boldsymbol{j}$ effect will do no net work. Nevertheless, it appears to be able to 'deflect' the electromotive force $\boldsymbol{u}\times\boldsymbol{B}$ from its former role, of generating toroidal field alone, to create poloidal field also. Certainly, despite the fact that in the case mentioned the new e.m.f. does no work, its presence seems to be sufficient to prevent the usual antidynamo proofs for symmetric fields from applying. And the numerical evidence for dynamos of the type appears convincing.

PHILOSOPHICAL TRANSACTIONS OF THE ROYAL SOCIETY A MATHEMATICAL, PHYSICAL & ENGINEERING SCIENCES

It may be argued that it is strictly inconsistent to include in (6.1) only that part of the deformation of the mean flow which is associated with rotation: the electromotive influence of the mean strain rates should also be included (Krause 1967). The main interest attaches, however, to the case in which the mean motion is nearly that of solid body rotation, i.e.

$$\boldsymbol{u} = \bar{\boldsymbol{\Omega}} \times \boldsymbol{r} + \boldsymbol{u}_1, \tag{6.11}$$

where $|u_1| \ll \bar{\Omega} a$. In the case of axisymmetric fields with cylindrical polar components of

$$\boldsymbol{B} = \left[-\frac{1}{\varpi}\frac{\partial P}{\partial z}, T, \frac{1}{\varpi}\frac{\partial P}{\partial \varpi} \right], \tag{6.12}$$

Ohm's law (6.2) becomes (in the leading approximation in $u_1/\bar{\Omega} a$)

$$\boldsymbol{j} = \sigma_T \left[\operatorname{grad} (\bar{\Omega} P - 2\beta_2 \bar{\boldsymbol{\Omega}} \cdot \boldsymbol{B}) + \boldsymbol{u}_1 \times \boldsymbol{B} - 2\bar{\Omega}\beta_1 \frac{\partial \boldsymbol{B}}{\partial z} \right]. \tag{6.13}$$

TABLE 9. MARGINAL REYNOLDS NUMBERS FOR THE RÄDLER $\boldsymbol{\omega} \times \boldsymbol{j}$ DYNAMO

The Reynolds numbers given by Rädler are $-2R^2$, where R is the Reynolds number listed below. Values marked with an asterisk were verified by the QR algorithm. Those listed for $M = \infty$ were obtained by an independent program which expanded eigenfunctions in series in r.

truncation		dipole				quadrupole		
N	M	first eigenvalue	second eigenvalue	third eigenvalue	Rädler value	first eigenvalue	second eigenvalue	Rädler value
1	20	16.04	33.47*	—	16.09	12.26	28.20*	12.26
1	∞	16.077	33.664	—	—	12.259	28.245	—
2	20	8.716	18.27*	—	18.31	8.413	17.89*	9.482
2	∞	—	—	—	—	8.4125	17.892	—
3	20	8.277	12.98*	16.73	16.79	8.097	12.33*	9.349
4	20	8.244	11.44*	17.64	16.20	8.075	11.15	9.130
5	20	8.243	11.20	14.76	16.10	8.074	10.97	9.125
6	20	8.243	11.18	14.05	16.09	8.074	10.96	9.123

The gradient term is, of course, ineffective and dynamo action must depend on the second and third terms on the right-hand side. If $\boldsymbol{u}_1$ is a differential rotation, the second term will fail without the third, and the discussion of the $\boldsymbol{\omega} \times \boldsymbol{j}$ dynamo above makes the third term seem unpromising in isolation. The governing equations now become ($\beta = \beta_1$)

$$\frac{\partial P}{\partial t} = \eta \Delta P - 2\bar{\Omega}\beta\varpi \frac{\partial T}{\partial z}, \tag{6.14}$$

$$\frac{\partial T}{\partial t} = \eta \Delta T + \frac{2\bar{\Omega}\beta}{\varpi}\frac{\partial}{\partial z}\Delta P + (\nabla \omega_0 \times \nabla P)_\phi, \tag{6.15}$$

where

$$\Delta = \varpi \frac{\partial}{\partial \varpi}\left(\frac{1}{\varpi}\frac{\partial P}{\partial \varpi}\right) + \frac{\partial^2 P}{\partial z^2} \tag{6.16}$$

and we have taken $\boldsymbol{u}_1 = \omega_0 \hat{\boldsymbol{z}} \times \boldsymbol{r}$. Defining R_ω to be the shear Reynolds number (4.1) as before, we see that, if

$$|R_\omega| \gg |R_\beta|, \tag{6.17}$$

where R_β is defined by (6.3) with $\omega = \bar{\Omega}$, the second term on the right of (6.15) may be neglected in comparison with the third. The critical Reynolds number upon which dynamo action depends is then

$$R = \sqrt{(|R_\omega R_\beta|)}. \tag{6.18}$$

Steady dynamo action appears to be possible only if $R_\omega R_\beta$ is negative. The two smallest eigenvalues are listed in table 9 for both dipole and quadrupole families, and are compared with values

of $-2R^2$ given by Rädler (1969*b*, 1970). Our results were obtained by the Bullard–Gellman method, and served as another check of our program. The values given for $M = \infty$ were obtained by an independent series expansion method based on Rädler's formulation (1969*b*). The agreement with Rädler's values is disappointing,† although his general conclusion, that the dipole type solution is *less* easily excited to dynamo action than the quadrupole family, is confirmed, albeit in a less pronounced fashion. From the values shown, it would appear that for values of N of 4 and larger, Rädler accidentally obtained an approximation to the second eigenvalue of the dipole family.

TABLE 10. SEARCH FOR OSCILLATORY RÄDLER $\boldsymbol{\omega} \times \boldsymbol{j}$ DYNAMO

$M = 20$ in all cases: Ω is oscillation frequency.

truncation	dipole		quadrupole	
N	R	Ω	R	Ω
1	66.06	126.8	45.25	59.61
2	48.86	33.37	44.74	42.84
3	52.04	34.17	44.58	47.85
4	50.17	16.24	44.75	38.14
5	49.84	6.660	44.98	32.74

A search was made for oscillatory eigenvalues in the case of positive $R_\omega R_\beta$. The results are shown in table 10. The convergence is suggestive but not convincing.

When inequality (6.17) is not obeyed, R will depend on R_β/R_ω. A good idea of the general effect is obtained by considering the steady state forms of (6.14) and (6.15), which give

$$0 = \eta \Delta P - 2\bar{\Omega}\beta\varpi \frac{\partial T}{\partial z}, \tag{6.19}$$

$$0 = \eta \left[\Delta T + R_\beta^2 \frac{\partial^2 T}{\partial z^2}\right] + (\nabla\omega_0 \times \nabla P)_\phi. \tag{6.20}$$

The effect of the second term on the right of (6.15) is here seen to be that of increasing the diffusion of T in the z direction from η to $\eta(1 + R_\beta^2)$, and therefore of making dynamo action less effective. This was confirmed by numerical results not reported here.

7. INTEGRAL PROPERTIES OF THE MODELS

Any of the converged models described in previous sections yield a wealth of information which is difficult to comprehend fully. Some information is given by plotting field structures, as in figures 2 to 6, 10, 13 and 16, but for many purposes it is more convenient to have available a portmanteau description of each dynamo which lists its salient attributes, such as dipole or quadrupole moment, toroidal and poloidal field energies, etc. This was done for a number of cases, and the results are shown in table 11. In using this table, the following points may be noted.

Three linear properties of the field are listed: the maximum toroidal field strength, T_{m}, the maximum poloidal stream function, ψ_{m} [see (5.5)], and the dipole (D) or quadrupole (Q) moment, M, as appropriate. Four quadratic properties are listed; the energy in the toroidal and poloidal fields, E_{T} and E_{P}, and the dissipation rates associated with the toroidal and poloidal fields, D_{T} and D_{P}. Since the governing equations are linear, any linear quantity may be scaled

† *Note added in proof*, 11 *July* 1972: Dr Rädler has just informed me (private communication) that he has recently obtained results in substantial agreement with those given by me in table 9.

PHILOSOPHICAL TRANSACTIONS OF THE ROYAL SOCIETY A MATHEMATICAL, PHYSICAL & ENGINEERING SCIENCES

Table 11. Summary of properties of models

For explanation of column labels, see text.

definition of model						linear properties			quadratic properties			
eqn no.	sign $\alpha\omega'$	sol. type	circ. $10m$	R	Ω	T_m	$10\psi_m$	$10M$	E_T	$10^{-1}E_P$	$10^{-2}D_T$	$10^{-3}D_P$
4.3	+	D	0	87.1	68.8	2.1	35.	4.3	4.9	14.	8.0	23.
	+	Q	0	76.1	55.1	1.4	25.	8.3	2.8	6.3	3.3	8.3
	−	D	0	74.4	54.1	1.6	24.	4.8	4.1	2.9	5.6	3.5
	−	Q	0	85.4	67.4	2.1	22.	5.6	5.0	3.3	8.3	5.3
4.5	+	D	0	258.	66.6	5.2	18.	6.3	3.2	21.	5.4	41.
	+	Q	0	212.	49.7	3.0	11.	10.	1.7	6.6	1.9	9.8
	−	D	0	206.	47.4	3.9	12.	7.3	1.7	3.9	3.4	5.6
	−	Q	0	254.	68.5	6.0	12.	7.4	3.8	5.6	6.4	11.
5.1	+	D	5.0	63.6	0	2.3	7.8	7.1	1.2	4.6	2.2	4.7
	+	D	−3.1	31.5	0	2.2	8.3	8.5	1.4	2.8	1.0	1.2
	−	D	−5.5	82.4	0	2.0	8.6	7.9	1.5	7.0	2.7	9.4
	+	Q	−4.0	66.2	0	2.9	6.2	2.2	2.6	1.9	4.0	3.1
	+	Q	5.0	113.	0	2.4	6.9	2.4	2.1	2.8	4.0	7.4
	−	Q	4.0	32.1	0	2.6	5.5	4.1	1.8	2.2	9.4	1.7
	−	Q	−5.0	70.9	0	1.9	3.8	5.5	0.99	1.2	1.4	1.4
5.6	−	D	−1.59	118.	0	1.3	8.6	8.2	0.36	7.8	0.62	7.9
	−	Q	−2.04	71.9	0	1.8	6.4	8.7	1.3	3.9	0.92	3.0
	+	D	2.27	59.8	0	1.1	7.6	7.5	0.46	7.3	0.48	9.8
	+	Q	0.91	168.	0	3.1	12.	13.	1.9	5.8	2.0	3.8
5.7	+	D	3.41	79.9	0	0.74	7.7	7.4	0.17	8.4	0.38	12.
	+	Q	2.73	134.	0	2.3	9.1	2.0	3.2	3.5	5.3	5.3
	−	D	−3.07	67.8	0	1.4	8.4	9.0	0.80	5.1	0.96	3.9
	−	Q	−3.07	53.3	0	1.9	4.2	6.5	1.4	1.1	1.2	0.67
5.8	−	D	2.73	124.	0	1.3	8.0	4.9	0.37	9.6	0.77	19.
	+	D	1.36	68.3	0	1.8	7.9	8.7	0.66	4.1	0.82	2.3
	+	D	−2.05	86.1	0	1.4	8.0	8.8	0.78	5.3	0.79	4.5
	−	Q	2.73	173.	0	1.9	12.	2.1	1.5	8.8	2.3	12.
	+	Q	2.05	72.2	0	2.6	11.	15.	1.8	5.7	2.2	3.3
	+	Q	−2.39	82.5	0	2.3	6.9	9.9	2.0	4.2	1.1	3.3

up by a constant (k, say), provided the remaining linear properties are scaled up by the same factor, and the quadratic quantities are scaled up by k^2. Moreover, the transformation (4.7) may be applied to any $\alpha\omega$ model to obtain further useful information. It should be noted that (5.1) is used, rather than (5.2), to define the Braginskiĭ model. The value we obtain for the energy dissipation integral in the second case listed is of the same order of magnitude as the one he provides, but the agreement is not as satisfactory in detail as for the comparisons quoted in § 5. Finally, we may observe that, in the case of the oscillatory $\alpha\omega$ dynamos, the linear properties listed refer to the maximum modulus over a cycle, and the quadratic properties are avearges over a cycle. Twenty grid points were used, and $N = 8$ for the oscillatory solutions and $N = 9$ for the steady solutions.

8. Conclusions

This work was undertaken for a variety of reasons. First, there appeared to be some conflicting results in the literature. For example, an early study by Steenbeck & Krause (1966) indicated that the $\alpha\omega$ dynamos were typically steady (d.c.), and yet their later work (e.g. Steenbeck & Krause 1969*a*) suggested instead that they were more commonly oscillatory (a.c.); no satisfactory explanation was given. Again, the earlier paper implied that, for dynamos with the fundamental symmetry property (2.7), it might be possible to excite dipole and quadrupole fields with almost equal ease, and yet the later study reported that, in more than one case, the smallest Reynolds number for quadrupole excitation greatly exceeded that required for dipole regeneration.

As a result of the calculations of § 4, we conclude that each paper is correct in one respect, and incorrect in the other. In every case considered, the $\alpha\omega$ dynamo was oscillatory (see also the arguments of Weiss 1971), and the progression in the field patterns could be understood in terms of the dynamo waves of Parker (1955). In every case, however, the fields of dipole and quadrupole parity were (essentially) equally readily excited. There was a slight tendency for the a.c. dipole to be preferred over the a.c. quadrupole, provided $\alpha\omega'$ was negative in the northern hemisphere, and this may provide some grounds for believing that ω' increases with depth in the Sun (since α is very probably positive in its northern hemisphere). If, however, $\alpha\omega'$ were positive in the northern hemisphere, the a.c. quadrupole would be more readily excited than the a.c. dipole solution.

The surprisingly similar magnitude of the eigenvalues for dipole and quadrupole symmetries persists for the α^2 dynamos considered in § 3, and for the Rädler dynamos considered in § 6. It is destroyed when meridional circulations are present. In every case, there is then a preferred magnitude of meridional flow speed, m, for which the critical magnetic Reynolds number, R, is substantially smaller than for other values of m. The associated dynamo is invariably of d.c. type, and its parity depends crucially on the sign of $\alpha\omega'$. For the first three models of § 5, there was a strong tendency for the d.c. dipole to be preferred over the d.c. quadrupole, provided $\alpha\omega'$ was positive in the northern hemisphere, and this may provide grounds for believing that this is the state of affairs in the core of the Earth. If, however, $\alpha\omega'$ were negative in the northern hemisphere, the d.c. quadrupole would be more readily excited than the d.c. dipole solution. It may be noted that this preference is *opposite* to that of the a.c. $\alpha\omega$ dynamos. (The fourth model of § 5 showed similar behaviour, but the difference between the Reynolds numbers for the two parities at the most favourable m was not substantial.)

A new symmetry property may be noted. The minimum Reynolds number for the quadrupole type fields, most easily excited when $\alpha\omega' < 0$ in the northern hemisphere, is almost equal to the

minimum Reynolds number appropriate to the dipole type fields, most easily excited when $\alpha\omega' > 0$ in the northern hemisphere. The circulation speeds at which these minima in R occur are almost equal and correspond in order of magnitude to an overturning in one electromagnetic diffusion time. The direction is, however, opposite in the two cases. It appears to be subject to no general principle, but to depend on the distribution of inductive (α and ω) sources in the particular model under consideration. For example, in the Braginskiĭ model, the 'best' direction is that from equator to pole (for the most easily maintained dipole solution when $\alpha\omega' > 0$ in the northern hemisphere). For the other three cases considered in § 3, however, the circulation for the similar 'best' solution is in the opposite sense.

Palaeomagnetic data indicate that the geomagnetic field has always been predominantly dipolar rather than quadrupolar (Runcorn 1959), and one may surmise that this indicates that (unlike the solar convection zone) the Earth's core contains significant meridional circulations, possibly associated with Ekman pumping created by the mean azimuthal flow (Roberts 1967*b*). It is not clear why the sense and magnitude of this circulation should adjust itself to be the one most favourable for dynamo action, but one idea, originally proposed by Malkus, is a deep thermodynamic one: the magnetohydrodynamic state of the core (assumed, for arguments sake, to be driven by convection from an applied temperature contrast) 'adjusts itself' to maximize the heat transported across it. So far, there is little concrete evidence to support this attractive heuristic notion, but (if correct) it is significant that convection in a rapidly rotating fluid may be *facilitated* by the presence of a sufficiently strong magnetic field (see, for example, Roberts 1971*b*). From this point of view, the meridional circulation which can generate the magnetic field the most easily will be thermodynamically favoured.

I am grateful to Mr W. B. Frye for assistance with the visual display programs and to Dr G. O. Roberts for advising on the inverse iteration method. The comments in the text on the review by Weiss (1971) were based on a preprint kindly supplied by its author, and not on the final version of that article. I am grateful to Dr N. O. Weiss for private correspondence concerning some points of apparent conflict between that preprint and the present work.

References

Backus, G. E. 1958 *Ann. Phys.* **4**, 372.
Braginskiĭ, S. I. 1964*a* *Z. èksper. teoret. Fiz.* **47**, 1084 (trans. *Soviet Phys. JETP* **20**, 726).
Braginskiĭ, S. I. 1964*b* *Geomag. Aeron.* **4**, 732 (English **4**, 572).
Bullard, E. C. & Gellman, H. 1954 *Phil. Trans. R. Soc. Lond.* A **247**, 213.
Childress, S. 1967 Courant Institute Report AFOSR-67-1024, New York.
Childress, S. 1969 Théorie magnetohydrodynamique de l'effet dynamo. *Rep. Dép. Méch. Fac. Sci., Paris*, 1969.
Childress, S. 1970 *J. Math. Phys.* **11**, 3063.
Cowling, T. G. 1933 *Mon. Not. R. astr. Soc.* **94**, 39.
Gibson, R. D. & Roberts, P. H. 1969 *The application of modern physics to the Earth and planetary interiors* (ed. S. K. Runcorn), p. 571.
Krause, F. 1967 *Habilitationsschrift*, Jena.
Lilley, F. E. M. 1970 *Proc. R. Soc. Lond.* A **316**, 153.
Lortz, D. 1968 *Plasma Phys.* **10**, 967.
Moffatt, H. K. 1969 *J. Fluid Mech.* **35**, 117.
Parker, E. N. 1955 *Astrophys. J.* **122**, 293.
Parker, E. N. 1971*a* *Astrophys. J.* **163**, 255.
Parker, E. N. 1971*b* *Astrophys. J.* **164**, 491.
Parker, E. N. 1971*c* *Astrophys. J.* **165**, 139.
Rädler, K.-H. 1969*a* *Mber. dt. Akad. Wiss. Berl.* **11**, 194.
Rädler, K.-H. 1969*b* *Mber. dt. Akad. Wiss. Berl.* **11**, 272.

PHILOSOPHICAL TRANSACTIONS OF THE ROYAL SOCIETY A MATHEMATICAL, PHYSICAL & ENGINEERING SCIENCES

Rädler, K.-H. 1970 *Mber. dt. Akad. Wiss. Berl.* **12**, 468.
Roberts, P. H. 1967 *a* *An introduction to magnetohydrodynamics*. London: Longmans, Green.
Roberts, P. H. 1967 *b* In *Woods Hole Oceanogr. Inst. Rep.* 67-54, pt. 1.
Roberts, P. H. 1971 *a* *The World magnetic survey* (ed. A. J. Zmuda), p. 123. IUGG Publication.
Roberts, P. H. 1971 *b* In *Lectures in applied mathematics*, **14** (ed. W. H. Reid), p. 129. American Mathematical Society.
Roberts, P. H. & Stix, M. 1971 The turbulent dynamo: a translation of a series of papers by F. Krause, K.-H. Rädler and M. Steenbeck. *Tech. Note* 1A-60 *Nat. Center Atmos. Res.*
Roberts, P. H. & Stix, M. 1972 *Astron. & Astrophys.* **18**, 453.
Runcorn, S. K. 1959 *J. atmos. terr. Phys.* **14**, 167.
Scott, S. 1969 Appendix to paper by Gibson & Roberts in *The applications of modern physics to the Earth and planetary interiors* (ed. S. K. Runcorn), p. 586. London: Wiley.
Soward, A. M. 1971 *J. Math. Phys.* **12**, 2052.
Soward, A. M. 1972 *Phil. Trans. R. Soc. Lond.* A, **272**, 431.
Steenbeck, M. & Krause, F. 1966 *Z. Naturf.* **21**, 1285.
Steenbeck, M. & Krause, F. 1969 *a* *Astr. Nachr.* **291**, 49.
Steenbeck, M. & Krause, F. 1969 *b* *Astr. Nachr.* **291**, 271.
Weiss, N. O. 1971 *Qu. Jl. R. astr. Soc.* **12**, 432.

PHILOSOPHICAL TRANSACTIONS OF THE ROYAL SOCIETY A MATHEMATICAL, PHYSICAL & ENGINEERING SCIENCES